Physics 610

Adv Particle Physics

April 2014

Detectors

- Interaction of Charged Particles and Radiation with Matter
  - Ionization loss of charged particles ✓
  - Coulomb scattering ✓
  - Radiation loss by electrons ✓
  - Absorption of γ -rays in Matter ✓
- Detectors of Single Charged Particles
  - Pictorial Detectors: Cloud Chambers, Emulsions, Streamer Chambers, Spark Chambers, Bubble chambers
  - Proportional counters, Drift chambers, Scintillation counters, Cerenkov counters, Solid-state counters,
- Shower Detectors and Calorimeters
  - Electromagnetic-shower detectors
  - Hadron-shower detectors

- References: Donald H. Perkins, Introduction to High Energy Physics, Fourth Edition

Spatial and Temporal Resolutions

Detector Type	Accuracy (rms)	Resolution Time	Dead Time
Bubble chamber	10 to 150 μm	1 ms	50 ms[a]
Streamer chamber	300 μm	2 μs	100 ms
Proportional chamber	$\geq$ 300 μm[b,c]	50 ns	200 ns
Drift chamber	50 to 300 μm	2 ns[d]	100 ns
Scintillator	—	150 ps	10 ns
Emulsion	1 μm	—	—
Silicon strip	$\frac{\text{pitch}}{3 \text{ to } 7}$ [e]	*f*	*f*
Silicon pixel	2 μm[g]	*f*	*f*

[a] Multiple pulsing time.

[b] 300 μm is for 1 mm pitch.

[c] Delay line cathode readout can give $\pm$150 μm parallel to anode wire.

[d] For two chambers.

[e] The highest resolution ("7") is obtained for small-pitch detectors ($\lesssim$25 μm) with pulse-height-weighted center finding.

[f] Limited at present by properties of the readout electronics. (Time resolution of $\leq$ 25 ns is planned for the ATLAS SCT.)

[g] Analog readout of 34 μm pitch, monolithic pixel detectors.

Pictorial Detectors

- Cloud chamber
  - condensation on track
- Emulsions
  - enhanced silver content, reveals (after development) particle tracks with extreme precision
- Streamer chambers
  - ionization of gas generates light through recombination which is photographed
- Spark chambers
  - breakdown through electrodes
- Bubble chambers
  - liquid is expanded to superheated condition

Bubble Chamber

- Invented in early 1950's by Glaser.
- Dominant detector for decades.
- Liquid at high pressure (5-20 atm.) is heated to just below boiling point.
- Sudden reduction of pressure puts liquid into superheated state and boiling begins along path of charged particle.
- Bubbles grow for a period of time (ms typically).
- Photograph and recompress.

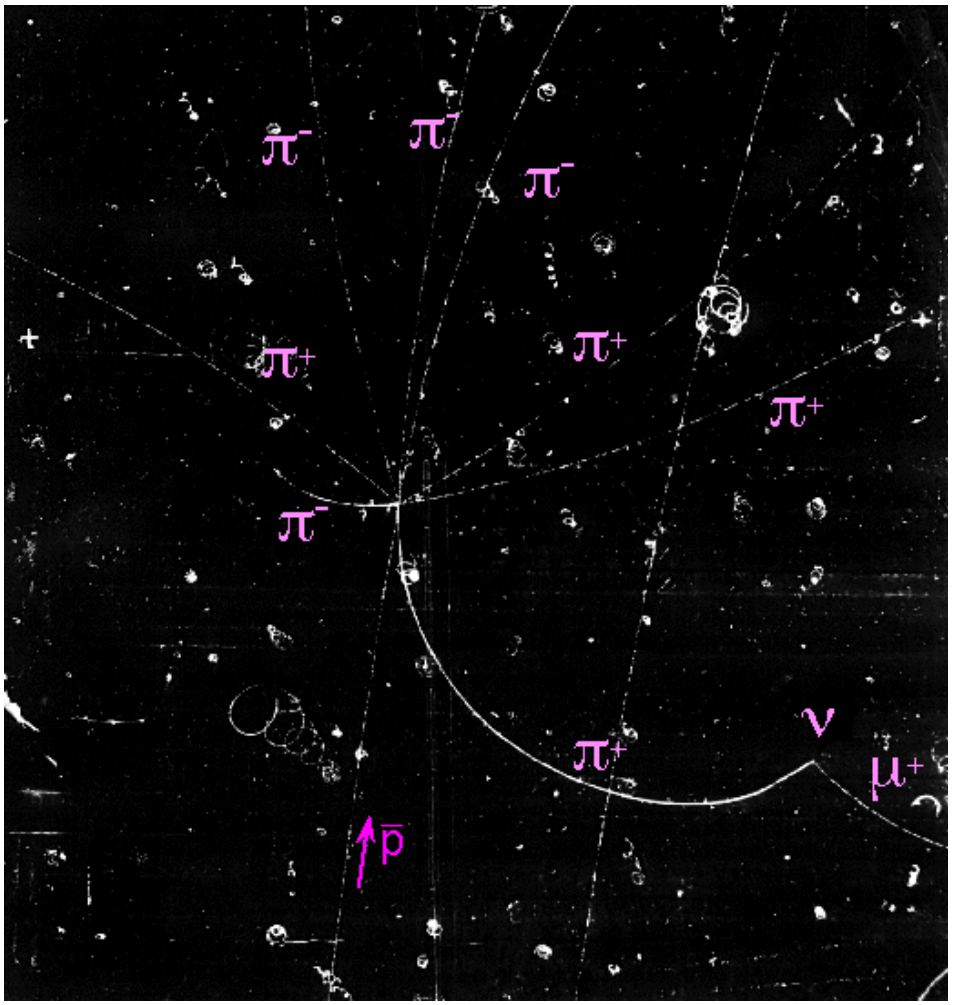

Bubble Chamber

- Several cameras provide stereo image
  - very detailed measurements following reconstruction
- Disadvantages
  - low repetition rate (1-20 Hz)
  - analysis of film complicated
  - very low duty cycle (~ 10^{-2})
  - not matched to colliding beam geometry

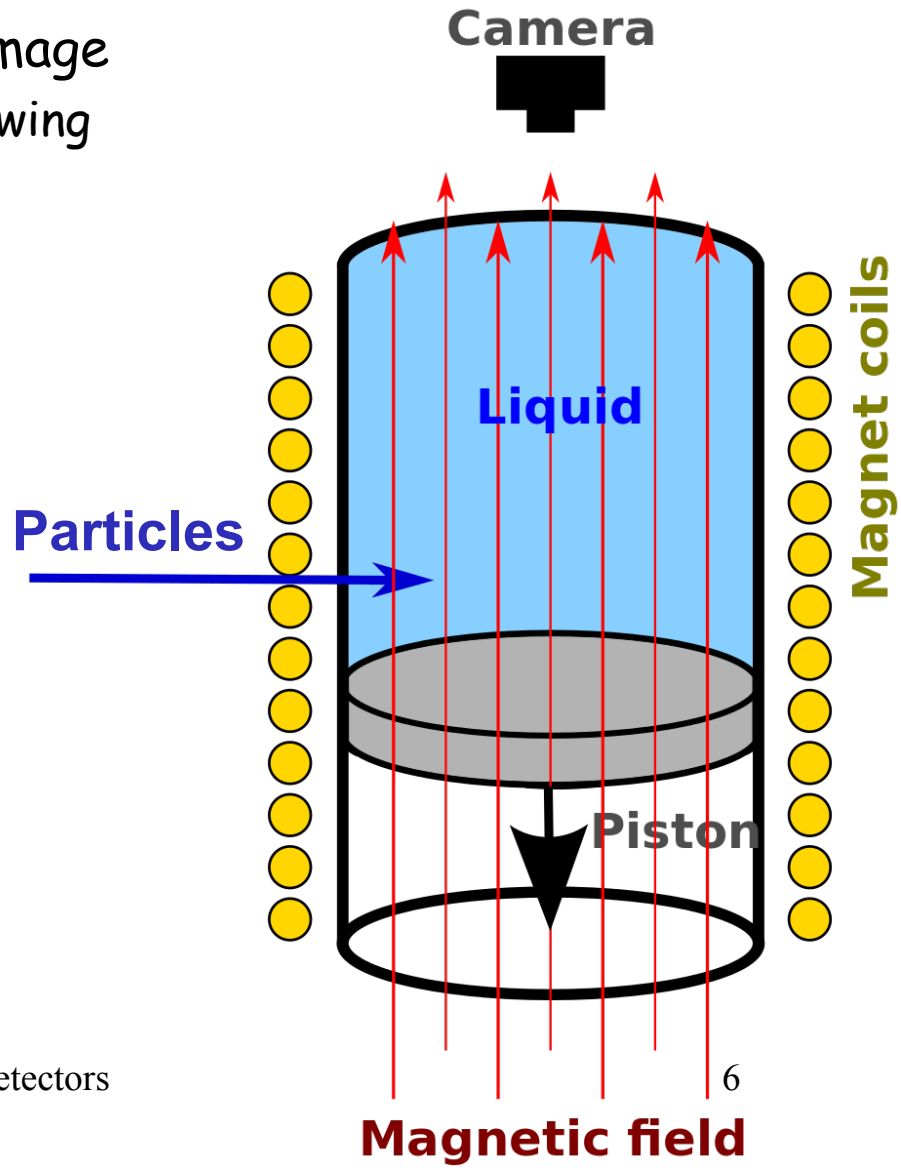

Bubble Chamber

- Liquids used
  - hydrogen - most elementary target material (proton)
  - deuterium - most elementary form of neutron targets
  - heavy liquids - short radiation length, or higher interaction rate

Table 2. Properties of bubble chamber liquid.

Liquid	Temperature	Density	Radiation length
	[K]	[g/cm^3]	[cm]
H2	25	0.0645	968
D2	30	0.14	900
Ne	35	1.02	27
He	3.2	0.14	1027
Xe	252	2.3	3.9
C_3H_8	333	0.43	110
CF_3Br	303	1.5	11
Ar	135	1.0	20
N_2	115	0.6	65

Gert G. Harigel, CERN

SLAC 1-meter Bubble Chamber

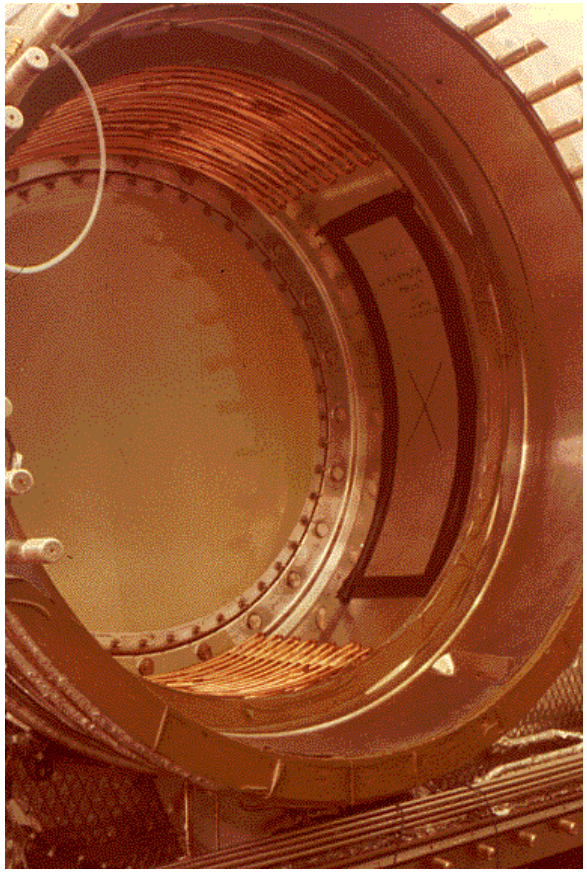

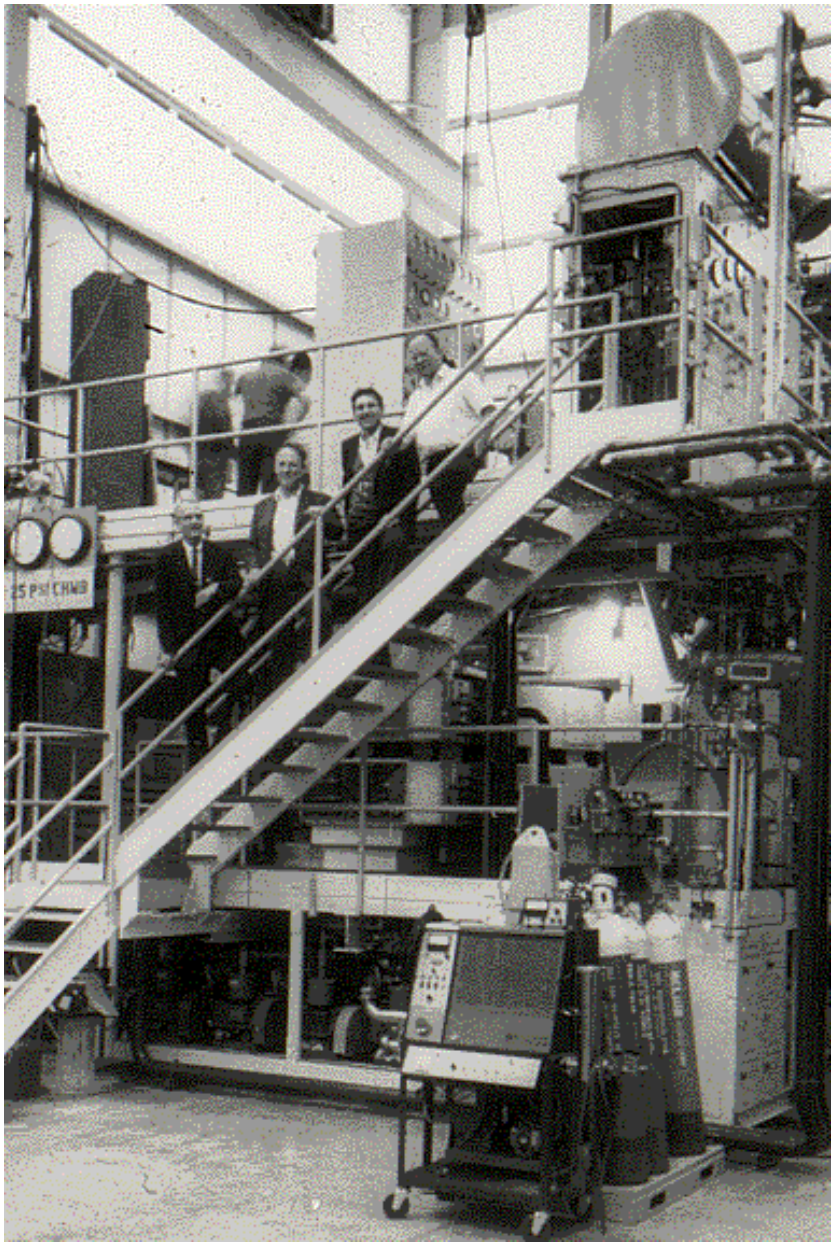

Bubble Chamber

- BEBC at CERN, 3.7 m diameter,
  - with EMI (MWPCs)
  - B = 2-3.5 Tesla

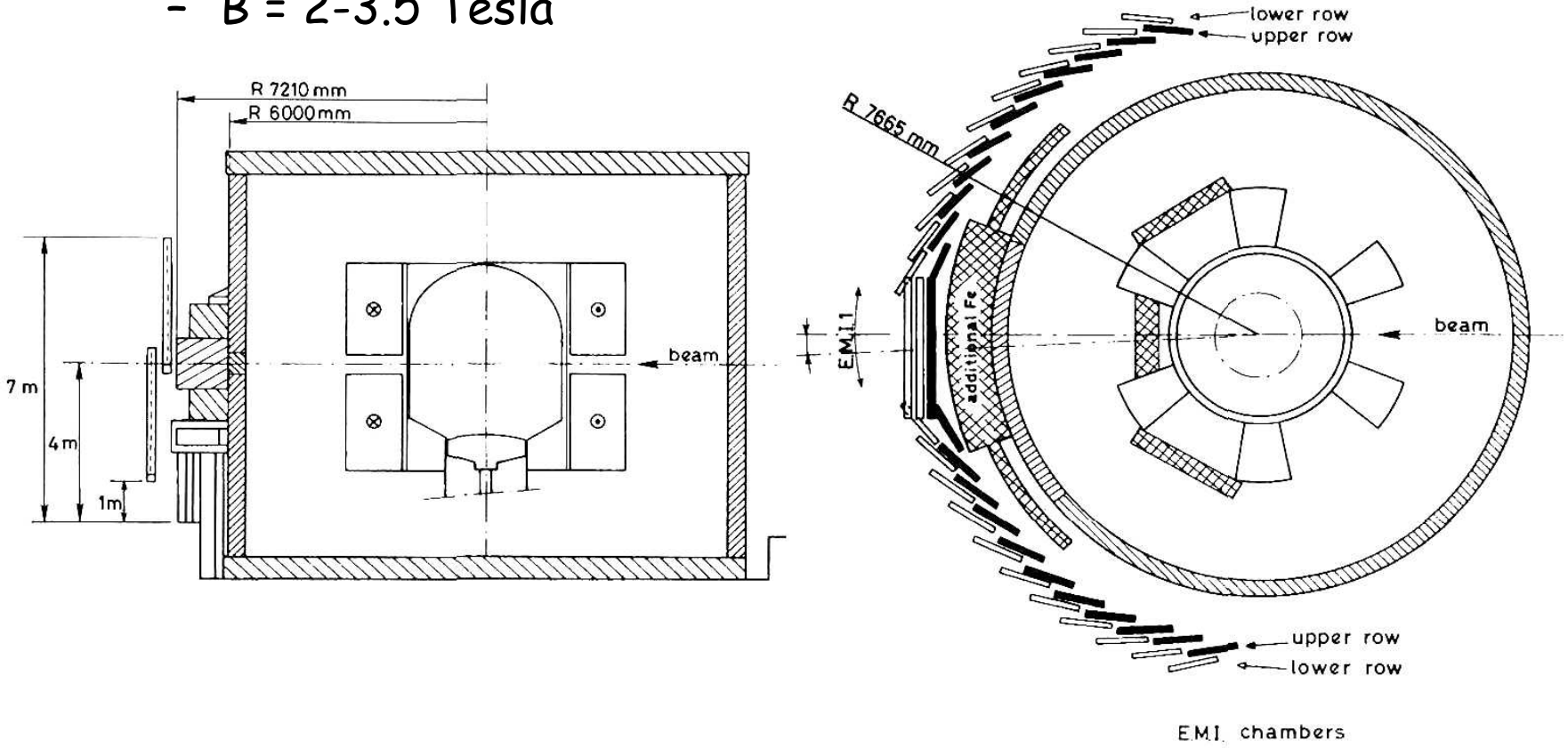

Bubble Chamber

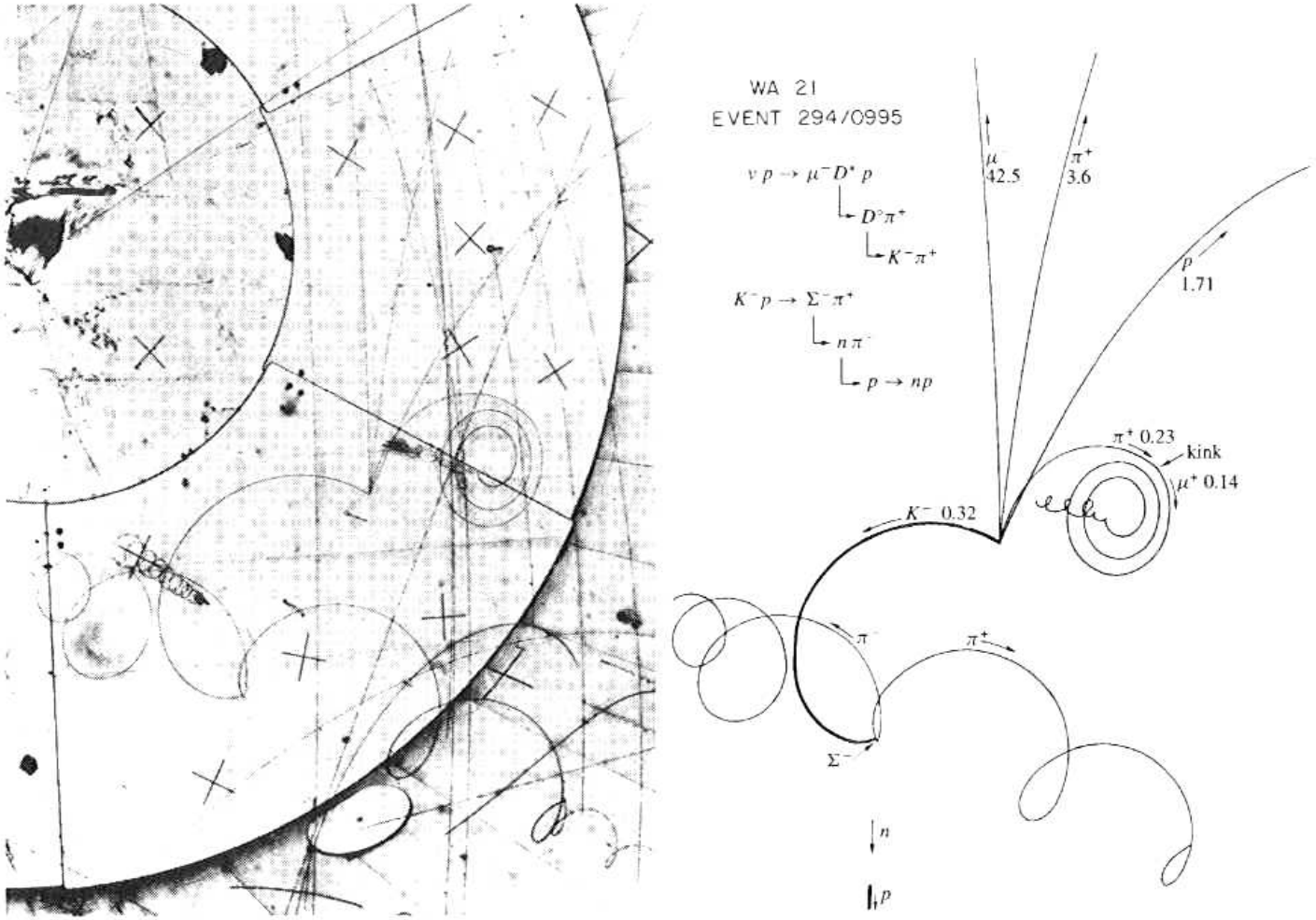

Hybrid Bubble Chamber

- Combine bubble chamber with a downstream system
- Example was the Fermilab 30-inch hybrid bubble chamber system
- Upstream measurements to tag beam particle
- Downstream measurement needed to achieve good momentum resolution on high energy tracks (beam momentum ~ 150 GeV/c)

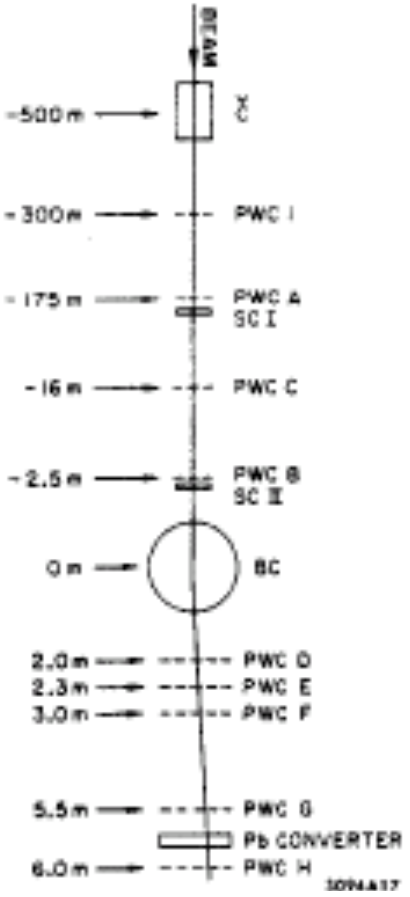

Triggered Bubble Chamber

- Use downstream system to trigger bubble chamber flash
- Only take picture when event, or selected event, occurs in BC
- Example was the SLAC Hybrid Facility (1 meter BC)

- $\pi^+ p \rightarrow K^+ X$
- Flash in 2.5 msec
- 40% of photos had event
- ~15/1 reduction in photos

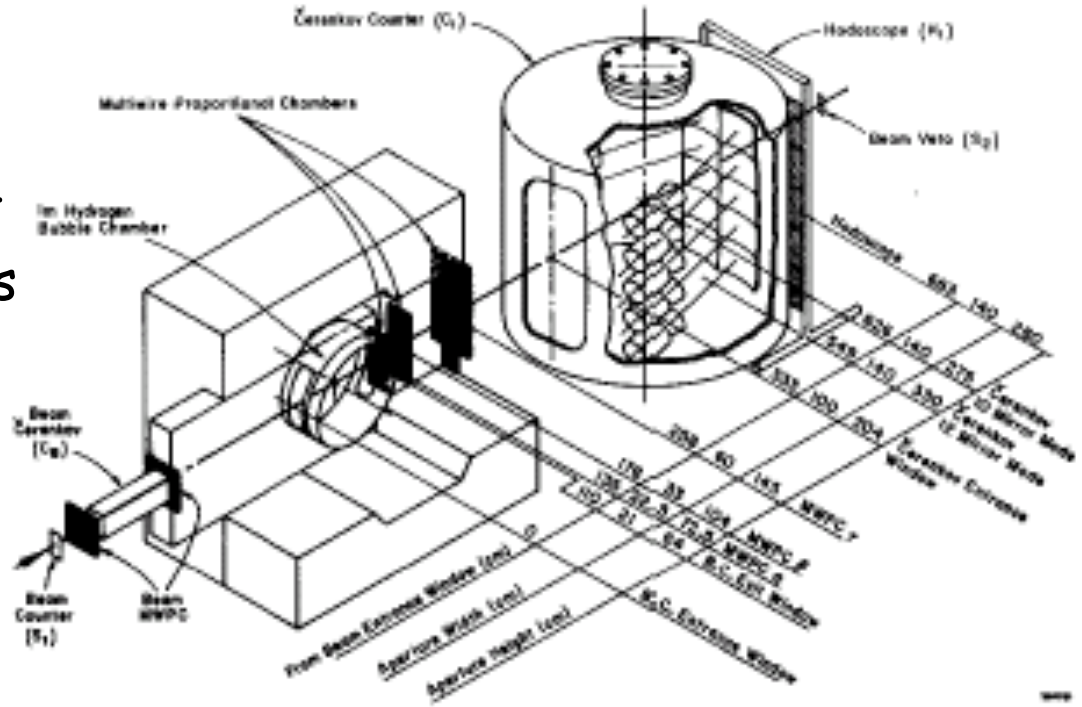

Triggered Bubble Chamber

- Event detected at SLAC 1 meter bubble chamber.
- Careful analysis shows this event is

$$\bar{p}\,p \rightarrow p\,\pi^{+}\,K^{-}\,\pi^{-}\,\pi^{0}\,K^{0}\,\bar{n}$$

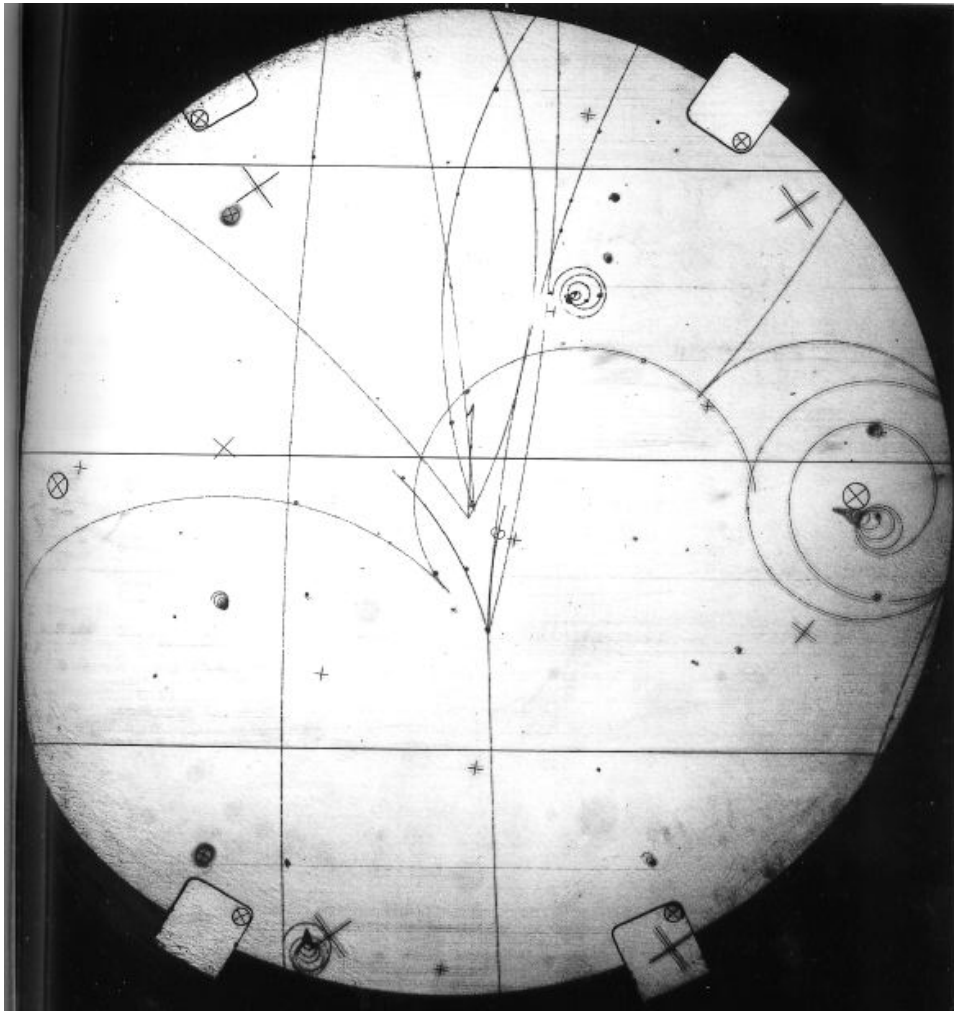

High Resolution Bubble Chamber

- Special optics were developed to improve resolution
  - Run bubble chamber "hot" (29K) to slow bubble growth and increase bubble density
  - Achieved bubble size of <50 μm (compared to standard ~300 μm)
  - Example, charm lifetime measurements in SLAC Hybrid Facility

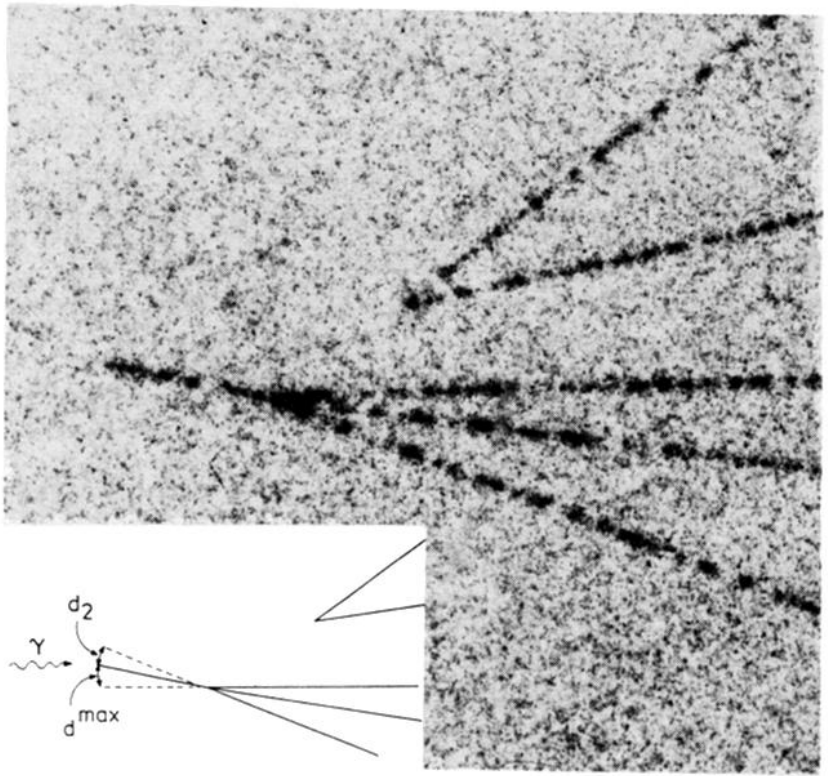

Decay lengths of
0.86 mm and 1.8 mm

Holographic Bubble Chamber

- In a conventional optics system the depth of field is coupled with the resolution:
  - DOF ~ λ / D^2
  - Resolution ~ λ / D
- Therefore, high resolution implies limited depth of field, reducing useful volume of bubble chamber
- A holographic system uncouples DOF and resolution
  - DOF ~ laser coherence length
  - Resolution ~ λ / D where D is the size of the recording medium
- Applied in two experiments at Fermilab in search of tau neutrino interactions in 1980s
  - Sensitive to large volumes – critical for neutrino experiments

Spatial and Temporal Resolutions

Detector Type	Accuracy (rms)	Resolution Time	Dead Time
Bubble chamber	10 to 150 μm	1 ms	50 ms[a]
Streamer chamber	300 μm	2 μs	100 ms
Proportional chamber	$\geq$ 300 μm[b,c]	50 ns	200 ns
Drift chamber	50 to 300 μm	2 ns[d]	100 ns
Scintillator	—	150 ps	10 ns
Emulsion	1 μm	—	—
Silicon strip	$\frac{\text{pitch}}{3 \text{ to } 7}$ [e]	*f*	*f*
Silicon pixel	2 μm[g]	*f*	*f*

[a] Multiple pulsing time.

[b] 300 μm is for 1 mm pitch.

[c] Delay line cathode readout can give $\pm$150 μm parallel to anode wire.

[d] For two chambers.

[e] The highest resolution ("7") is obtained for small-pitch detectors ($\lesssim$25 μm) with pulse-height-weighted center finding.

[f] Limited at present by properties of the readout electronics. (Time resolution of $\leq$ 25 ns is planned for the ATLAS SCT.)

[g] Analog readout of 34 μm pitch, monolithic pixel detectors.

Electronic Detectors

- Scintillators
- Proportional counters
- Multi-wire proportional counters
- Wire drift chambers
- Time projection chamber

Scintillators

- Certain materials scintillate when excited by ionizing particles
- Rutherford had his grad students counting the scintillations from zinc-sulfide
- Plastic or polystyrene are in common use today, but other material scintillate as well
- Organic
  - crystalline
  - liquid
  - plastic
- Inorganic

Scintillator Mechanism

- Scintillation:
  - Molecules are excited by a passing charged particle.
  - Certain molecules will release a small fraction (~3%) of this energy as optical photons, in a process known as scintillation.
  - Scintillation is particularly important in organic substances which contain aromatic rings, such as polystyrene, polyvinyltoluene, and napthalene.
  - Liquids which scintillate include toluene and xylene.

PDG

Scintillator Mechanism

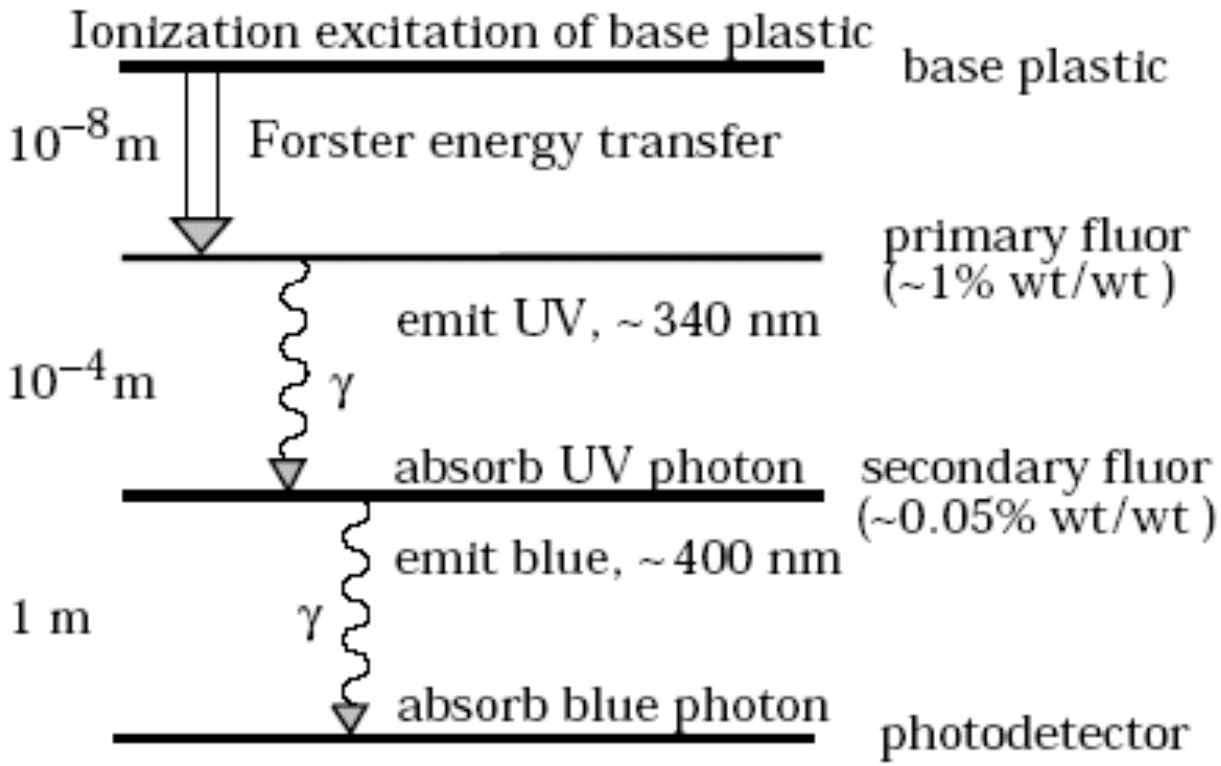

- Fluors
  (a) increase wavelength,
  (b) extend range of photons, and
  (c) speed up decay time

PDG

Fluorescence

- Fluorescence:
  - In fluorescence, the initial excitation takes place via the absorption of a photon, and de-excitation by emission of a longer wavelength photon.
  - Fluors are used as “waveshifters" to shift scintillation light to a more convenient wavelength.
  - Occurring in complex molecules, the absorption and emission are spread out over a wide band of photon energies, and have some overlap, that is, there is some fraction of the emitted light which can be re-absorbed.
  - This “self-absorption" is undesirable for detector applications because it causes a shortened attenuation length.

PDG

Scintillators

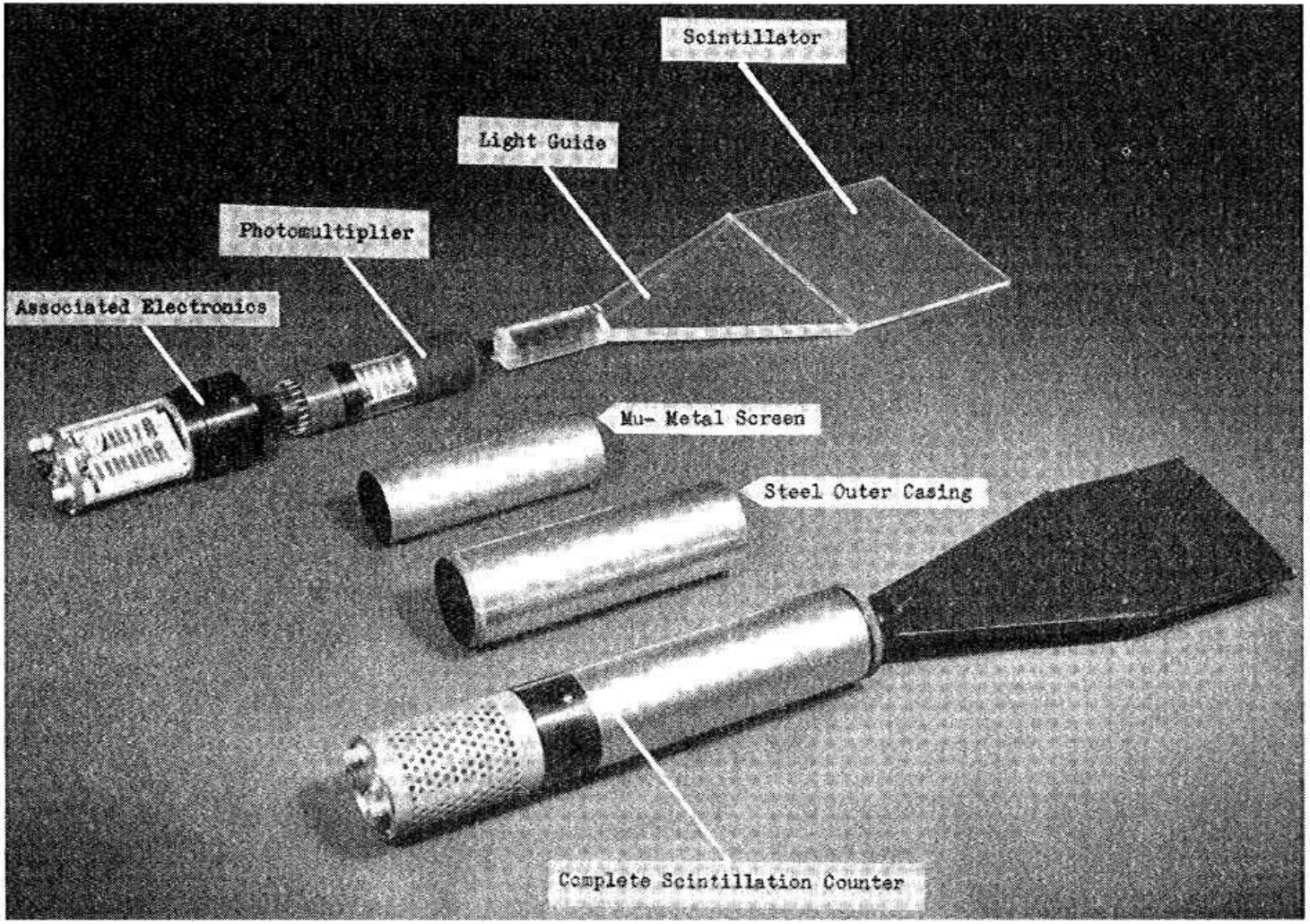

Organic Scintillators

- Most applications in HEP are plastic or liquid
- wide range of applications, extremely versatile

	Pulse height (relative to anthracene)	Decay time, ns	λ_{max}, Å	Density, g cm^{-3}
polystyrene + *p*-terphenyl	0.28	3	3550	0.9
polystyrene + tetraphenylbutadiene	0.38	4.6	4800	0.9
sodium iodide (+ thallium)	2.1	250	4100	3.7
anthracene	1.0	32	4100	3.7
toluene	0.7	<3	4300	0.9

Plastic Scintillators

- Plastic scintillators are reliable, robust, and convenient, but there are issues that must be dealt with
  - aging and handling
    - exposure can reduce light yield, and surface crazing destroys light transmission
  - attenuation length
    - care must be taken to ensure good transmission
  - afterglow
    - long-lived luminescence
  - atmospheric quenching
    - decrease light yield
  - magnetic field
    - small effects on light yield
  - radiation damage
    - reduced light yield, and attenuation length

Non-linear Response

- Plastic scintillators do not respond linearly to the ionization density.
  - Very dense ionization columns emit less light than expected on the basis of *dE/dx* for minimum ionizing particles.
  - A widely used semi-empirical model by Birks' posits that recombination and quenching effects between the excited molecules reduce the light yield.
  - These effects are more pronounced the greater the density of the excited molecules.
  - Birks ' formula is

$$\frac{d\mathscr{L}}{dx} = \mathscr{L}_0 \frac{dE/dx}{1 + k_B\, dE/dx}$$

  - where $\mathcal{L}$ is the luminescence, $\mathcal{L}_0$ is the luminescence at low specic ionization density, and k_B is Birks' constant, which must be determined for each scintillator by measurement.

PDG

Inorganic Scintillators

Crystal	ρ (g/cm^3)	X_0 (cm)	$r_{\text{Molière}}$ (cm)	dE/dx (MeV/cm)	λ_I (cm)	τ_{decay} (ns)	λ_{max}	n_D	Rel. output*	Hygro?
NaI(Tl)	3.67	2.59	4.5	4.8	41.4	250	410	1.85	1.00	very
BGO	7.13	1.12	2.4	9.2	22.0	300	410	2.20	0.15	no
BaF_2	4.89	2.05	3.4	6.6	29.9	0.7^f	220^f	1.56	0.05^f	slightly
						620^s	310^s		0.20^s	
CsI(Tl)	4.53	1.85	3.8	5.6	36.5	1000	565	1.80	0.40	some
CsI(pure)	4.53	1.85	3.8	5.6	36.5	$10, 36^f$	305^f	1.80	0.10^f	some
						$36^f, 620^s$	$\sim 480^s$		0.20^s	
$PbWO_4$	8.28	0.89	2.2	13.0	22.4	5–15	$420–440^\dagger$	2.3	0.01	no
CeF_3	6.16	1.68	2.6	7.9	25.9	10–30	310–340	1.68	0.10	no

* For standard photomultiplier tube with a bialkali photocathode. See Ref. 27 for photo-diode results.

† Emission ~ 500 nm also possible due to crystal defects.

f = fast component, s = slow component

Photomultiplier Tubes

- Light from scintillator is usually recorded by photomultiplier tubes
- photcathode coated by alkali metals
- amplification through dynode chain
  - 10^8 for 14 dynodes
- transit time ~ 50 nsec
- jitter ~ nsec
- quantum efficiency ~25%

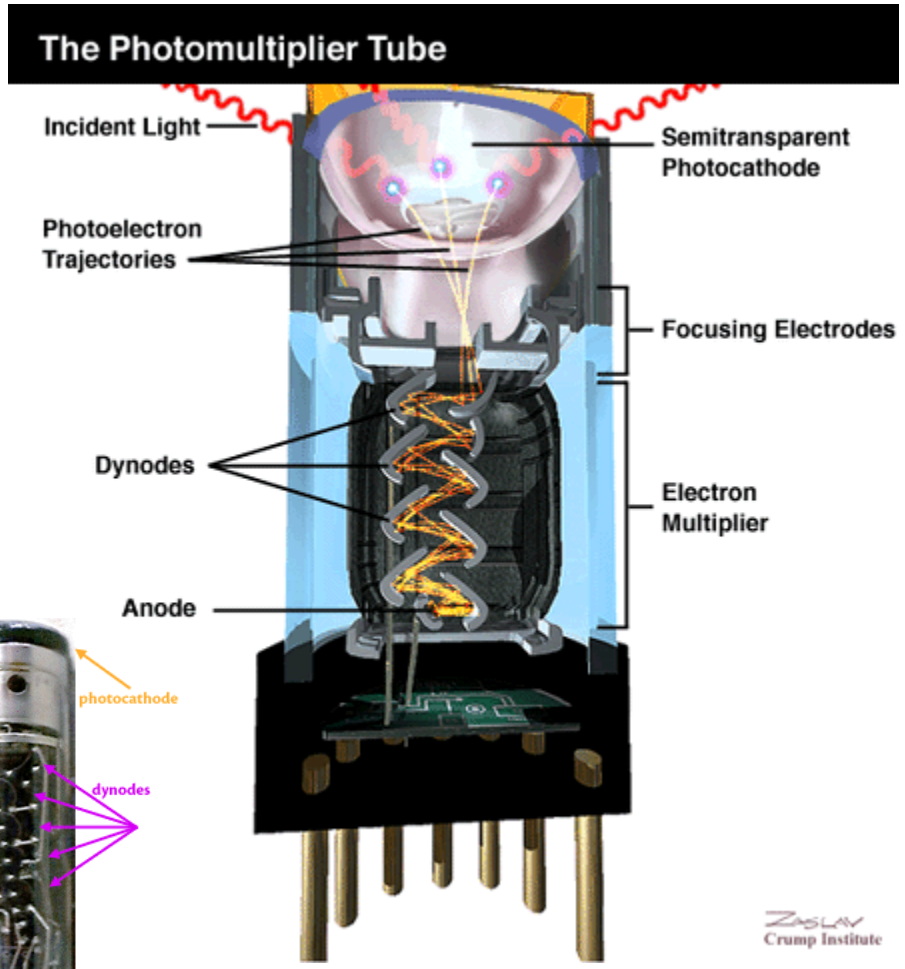

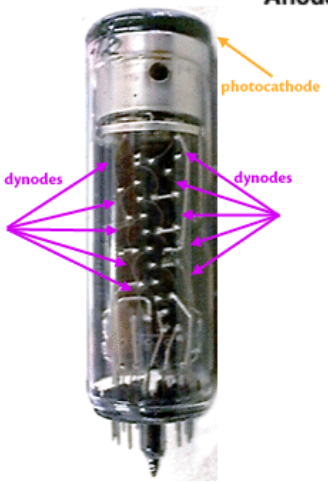

Typical Phototube - 931A

931A, 931B

Photomultiplier

28-mm (1-1/8 inch) Diameter 9-Stage,
Side Window PMTs

- Anti-Hysteresis Design
- Narrow Range of Anode Sensitivities
  931A: 30 A/lm - 600 A/lm
  931B: 100 A/lm - 1000 A/lm
- Low Dark Current

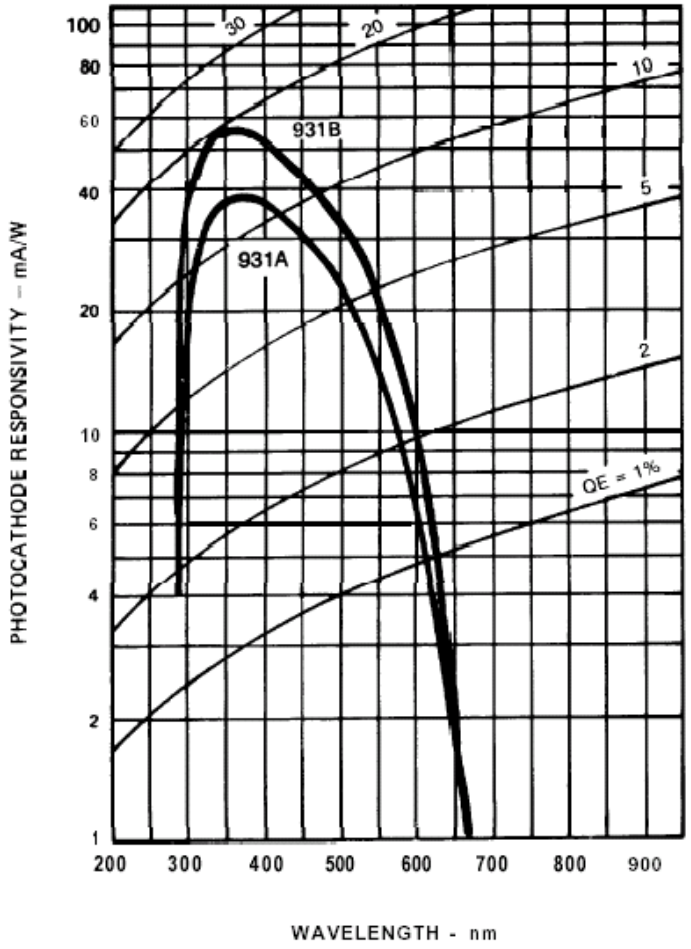

Figure 1 - Typical Photocathode Spectral Response Characteristics

Super K Phototubes

- Super Kamiokande
  - 11,146 tubes (20-inch diameter)

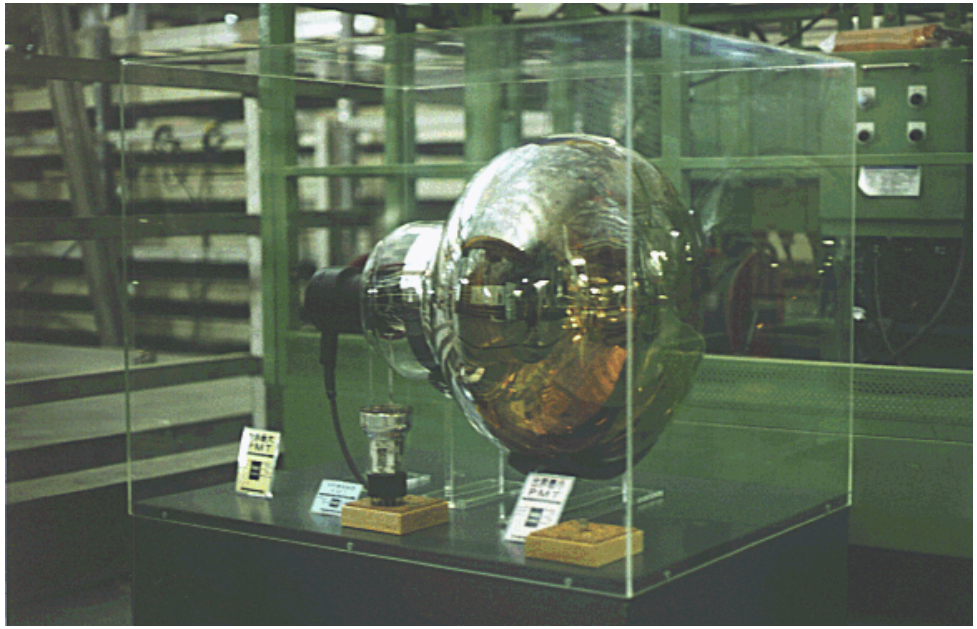

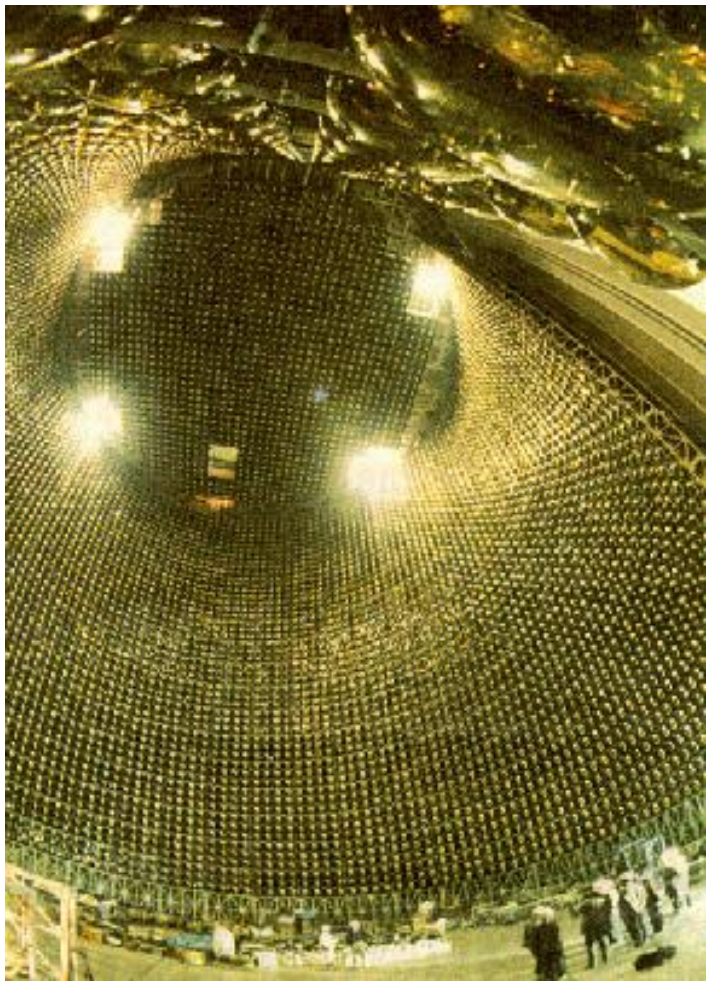

Photodiodes

- Higher quantum efficiency
- Lower power consumption
- More compact
- Improved ruggedness
- Immune to magnetic fields
- Good time response

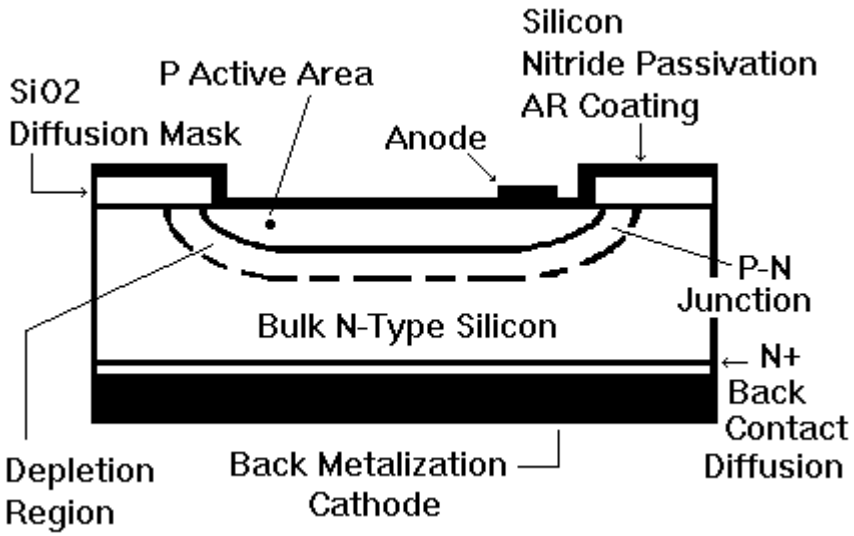

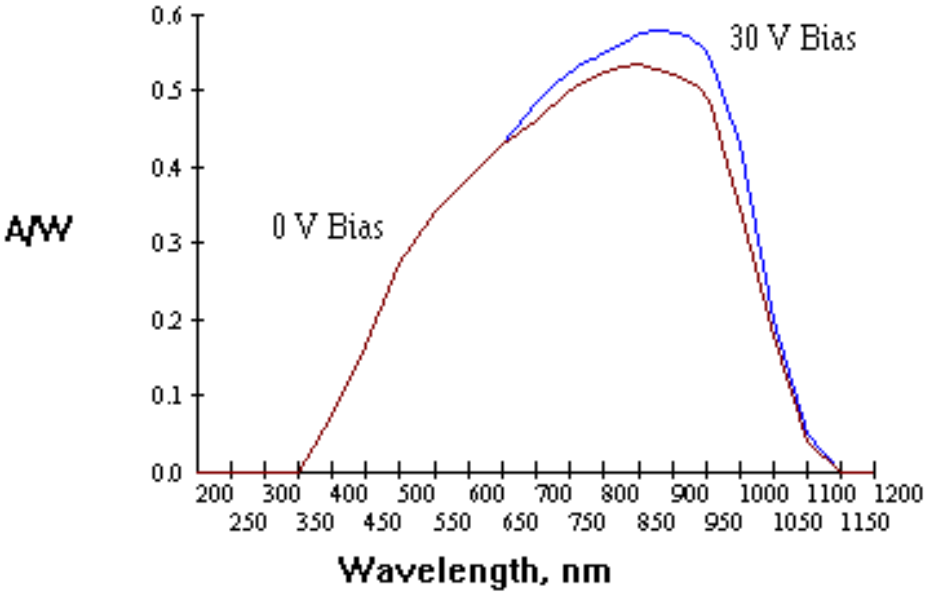

Light Path in Scintillator

- Light may be extracted from scintillator to phototube by internal reflection (multiple reflection down light guide)
- Alternative approach - wavelength shifter bars along edge of scintillator
  - blue light from scintillator re-emitted as green

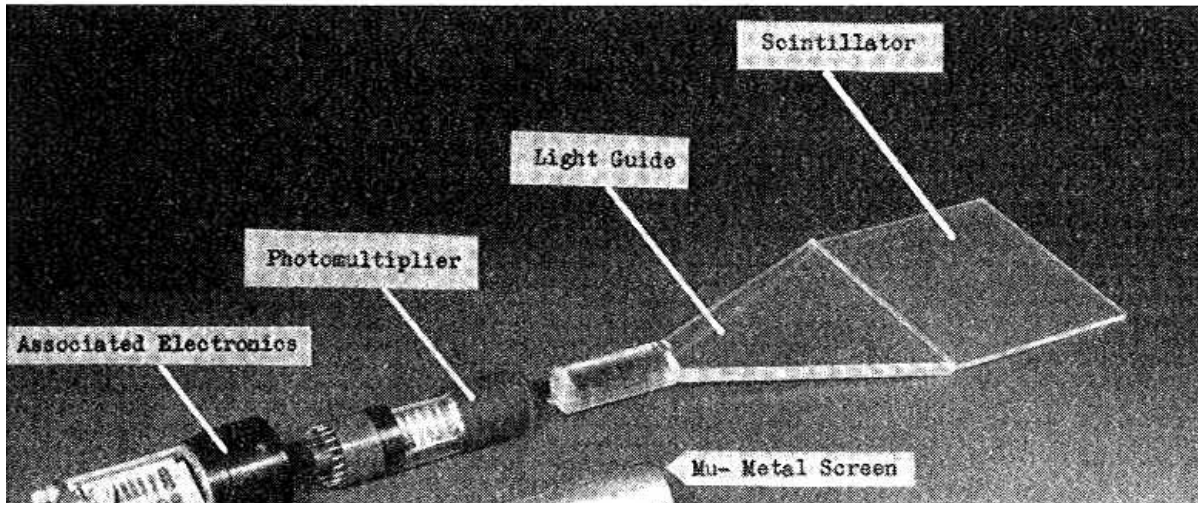

Proportional Counter

- Developed over a century ago
- Gas-filled cylindrical tube of radius r_2 at negative potential, with central anode wire of radius r_1 at positive potential

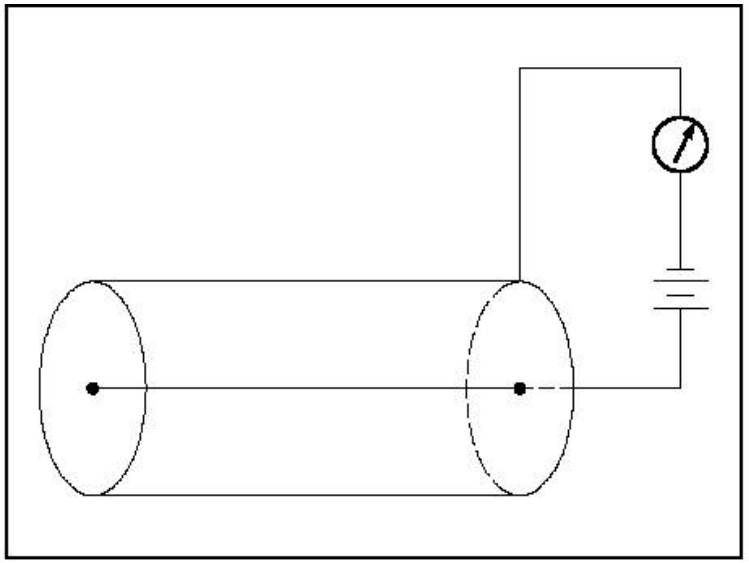

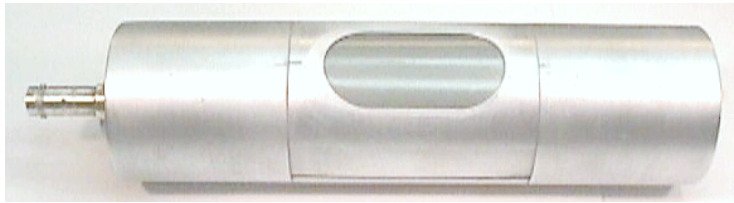

Proportional Counter

- For potential difference V_0, the electric field is

$$E(r) = \frac{V_0}{r \ln(r_2/r_1)}$$

- Liberated electrons drift toward anode, gaining energy.
- An avalanche is initiated if energy gain exceeds ionization energy
- Gas amplification of ~10^5 is typical, but independent of the number of primary ions "proportional counter"

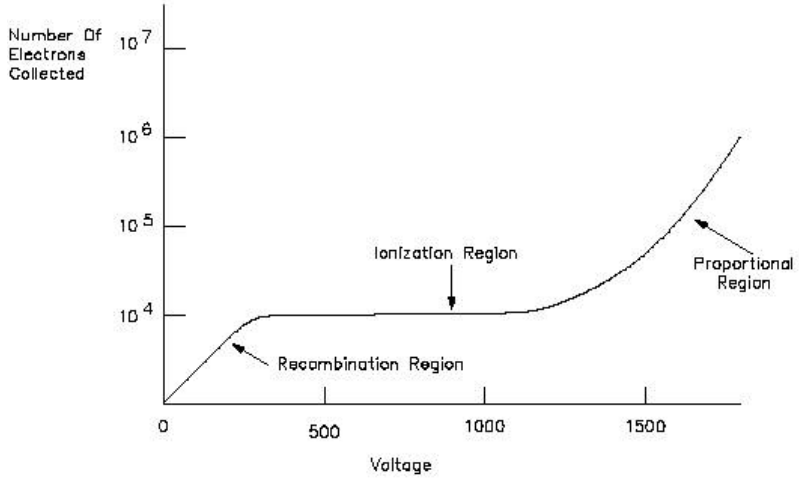

Multiwire Proportional Counter (MWPC)

- Around 1968, Charpak developed the MWPC
- Many parallel anode wires in a plane between two cathode planes
- Each wire is an independent detector
- Typical: 20 μm diameter wires, 5/cm, 12mm between cathodes, 5kV, argon-isobutane gas

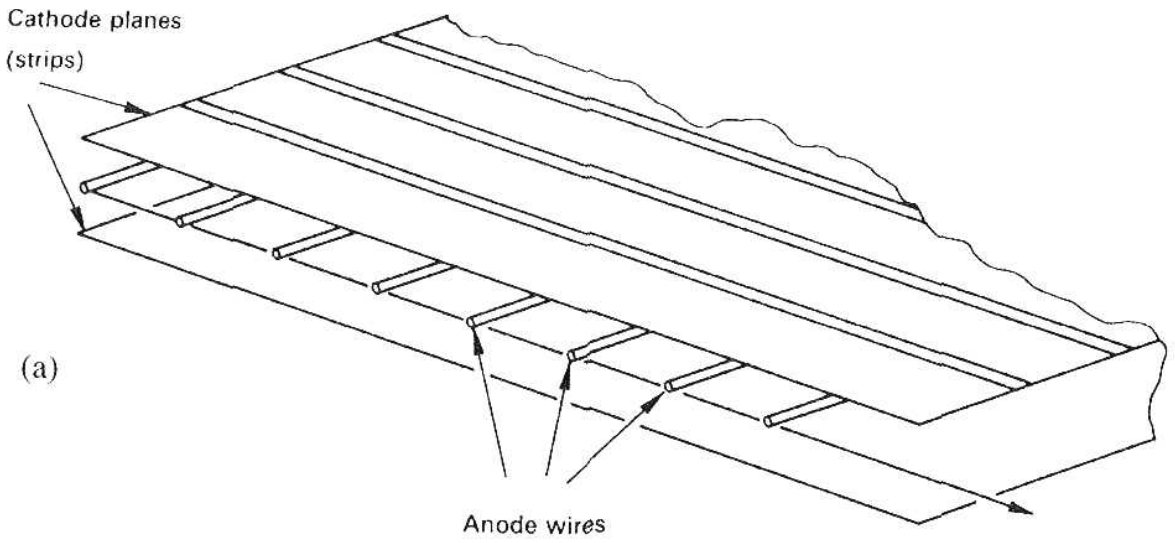

Multiwire Proportional Counter (MWPC)

- Electric Field Lines

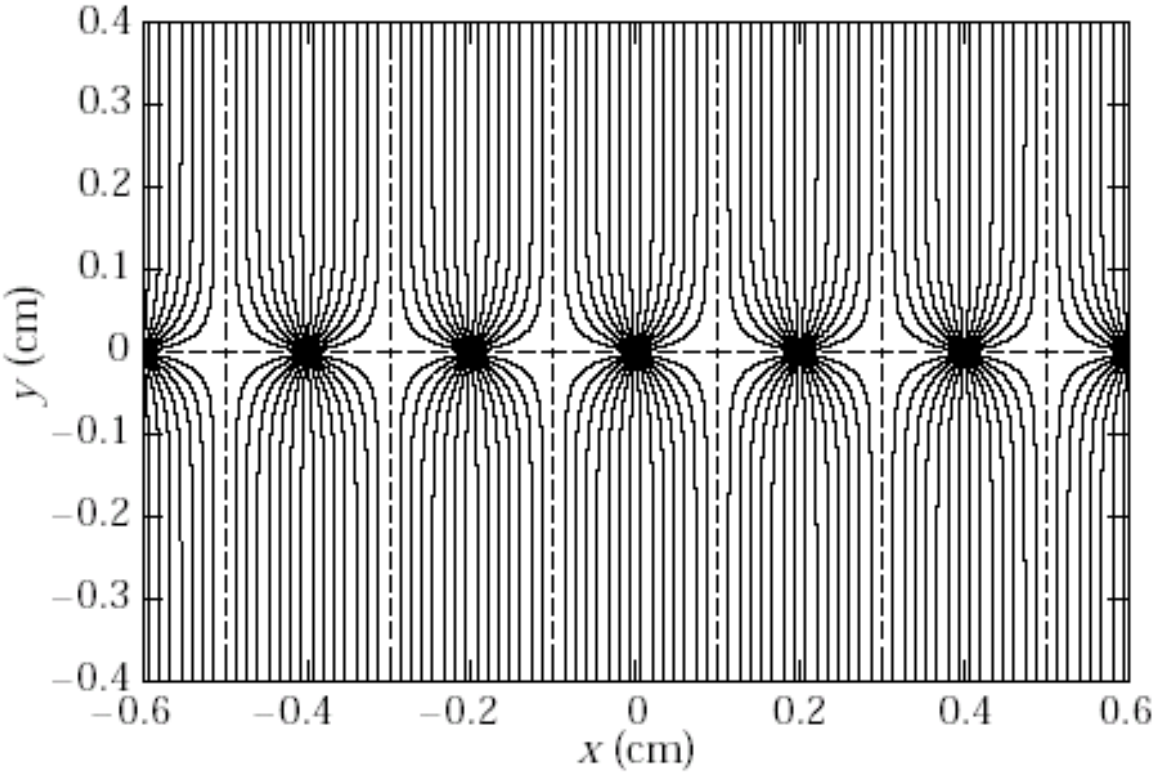

Multiwire Proportional Counter (MWPC)

- Fast rise time (0.1 nsec) arising from first arriving electrons
- Positive ions are slower, resulting in pulses of ~30 nsec duration
- Spatial resolution ~ 0.7 mm from anode pulses
- Cathode strips can be used to measure spatial coordinate of the avalanche (with about 0.05 mm precision)

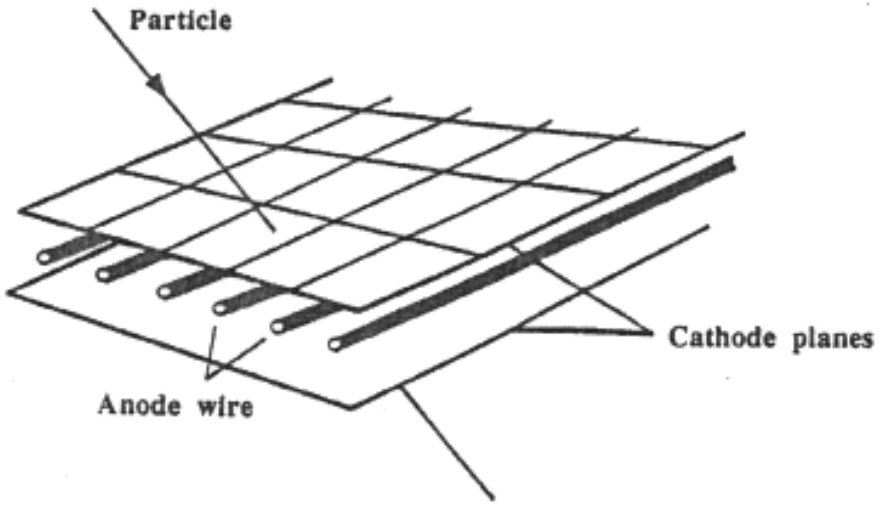

Wire Drift Chambers

- MWPCs require large number of wires and are limited to resolutions of about 1 mm and time resolutions of about 30 ns
- By drifting the charge, the number of wires can be significantly reduced, and the resolutions improved.
- Drift in field of ~ 1 kV/cm over 10 cm, amplify at anode
  - arrival time give measure of position

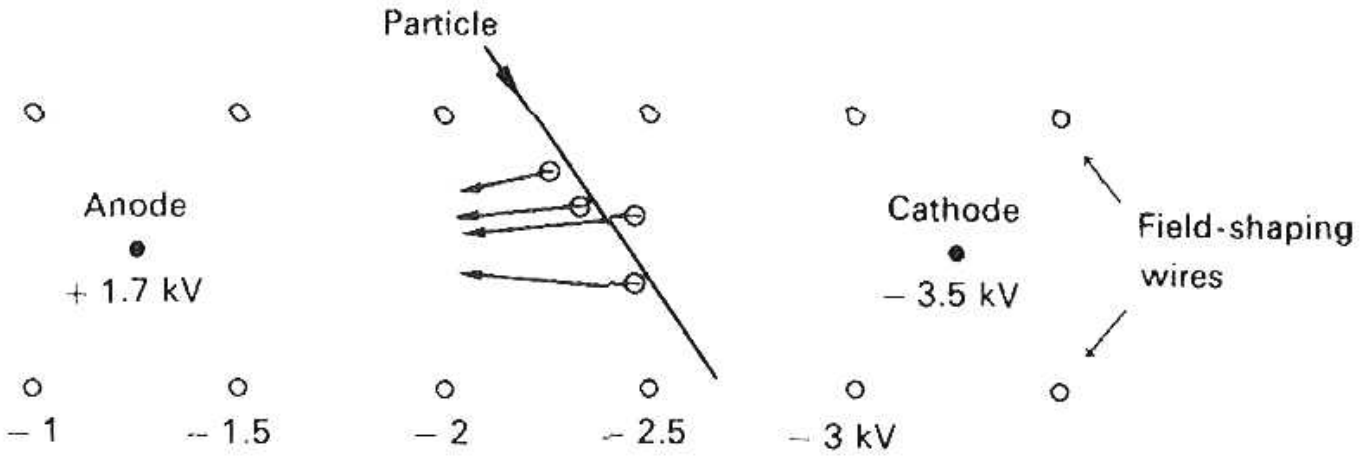

Wire Drift Chambers

- SLD Drift Chamber

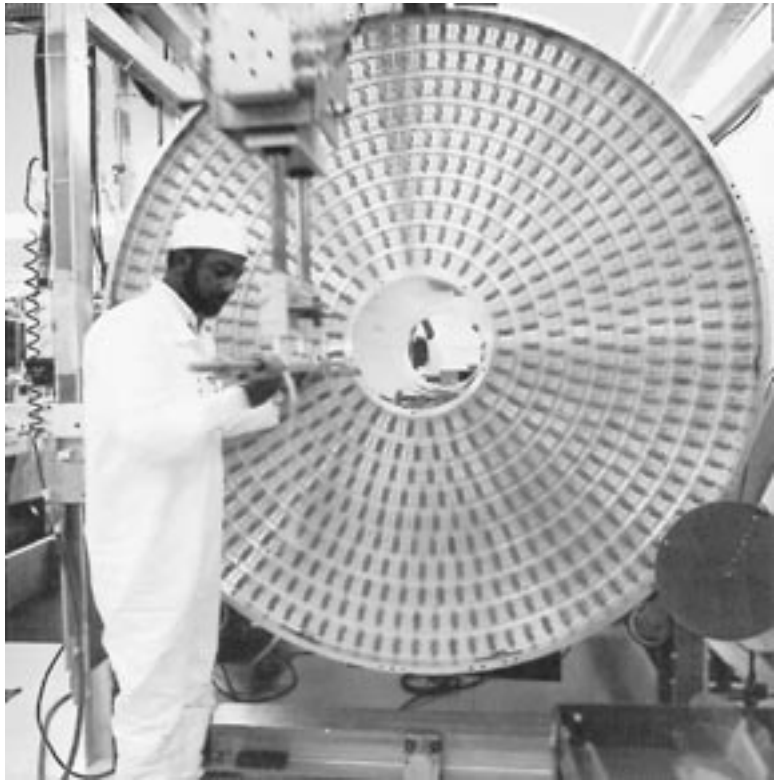

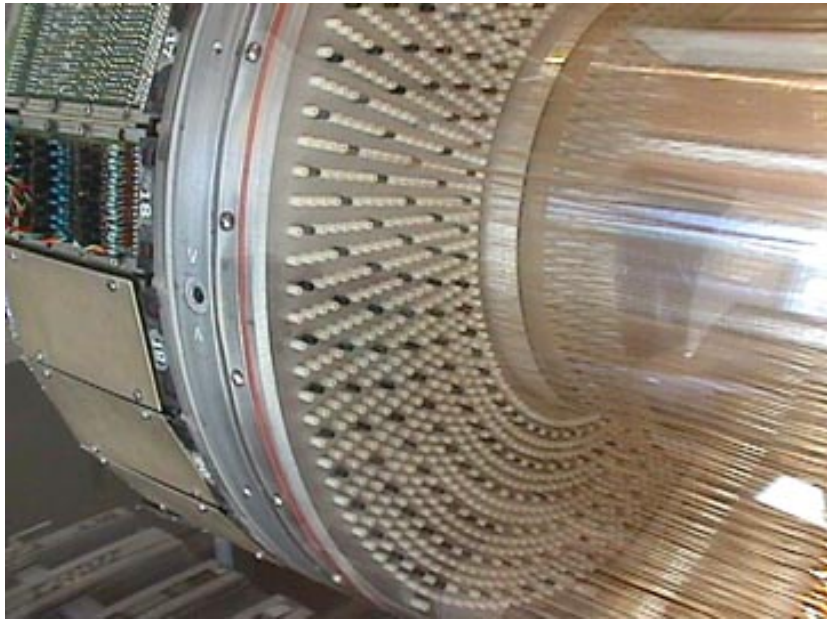

Wire Drift Chambers

- SLD Drift Chamber

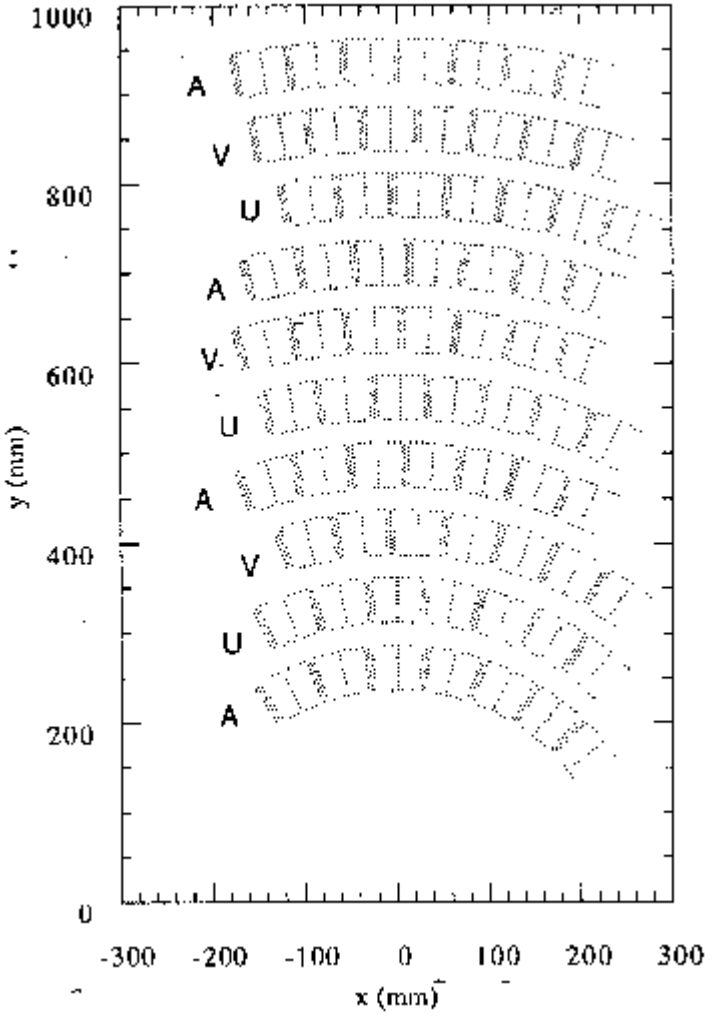

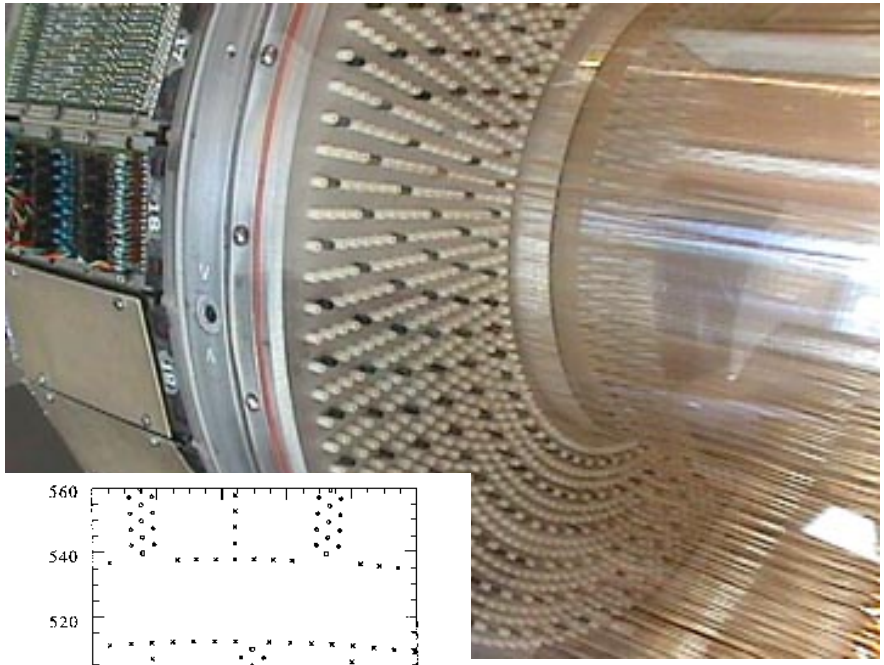

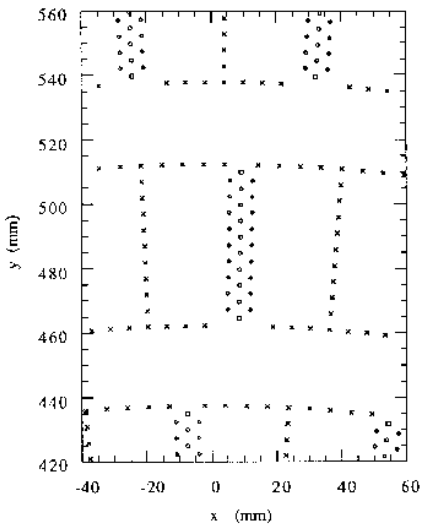

~100 μm resolution

Wire Drift Chambers

- SLD Drift Chamber

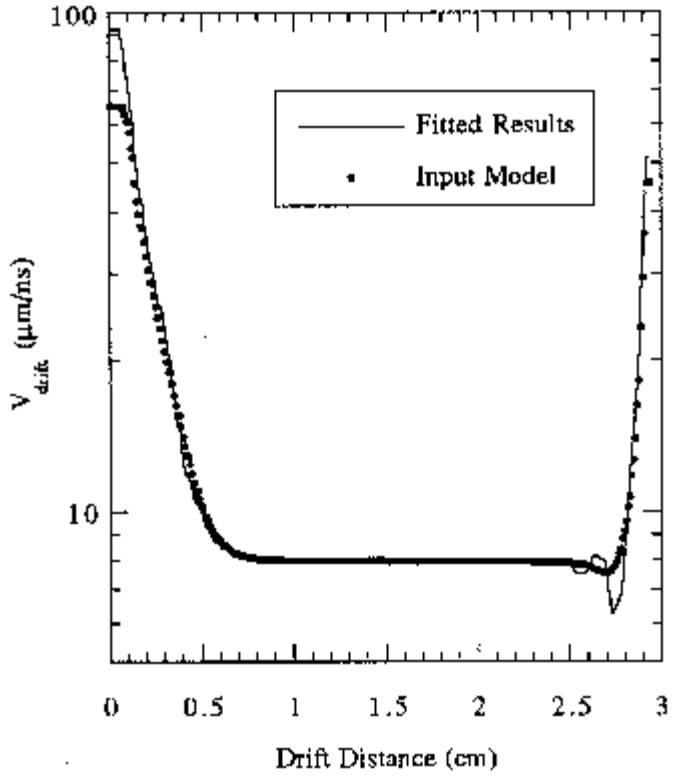

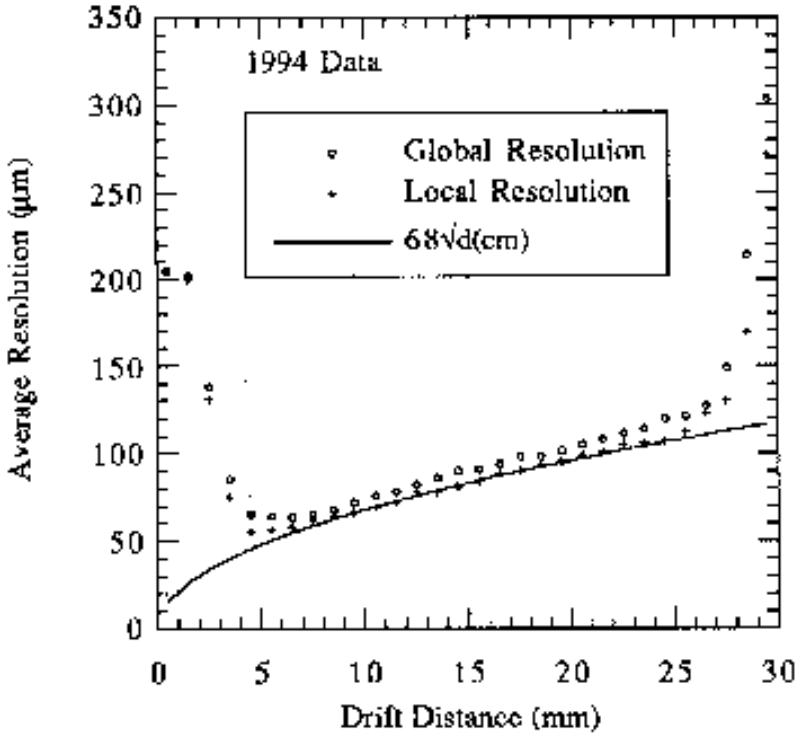

Time Projection Chamber

- Uniform electric field drifts ionization electrons to a 2D array of detectors at the end.
  - drift along the magnetic field direction to eliminate v x B force

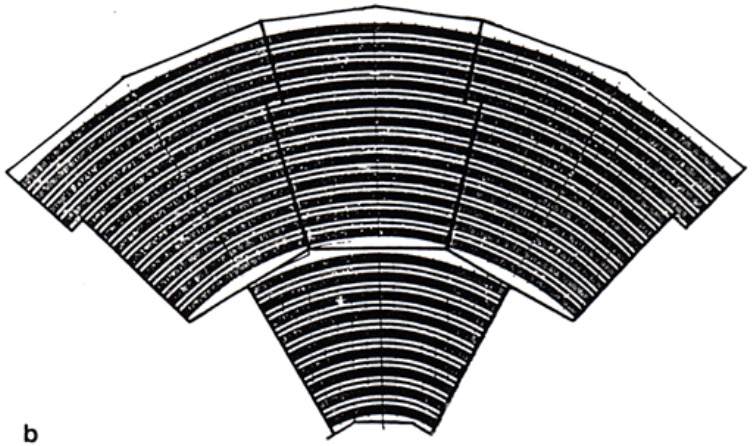

ALEPH TPC

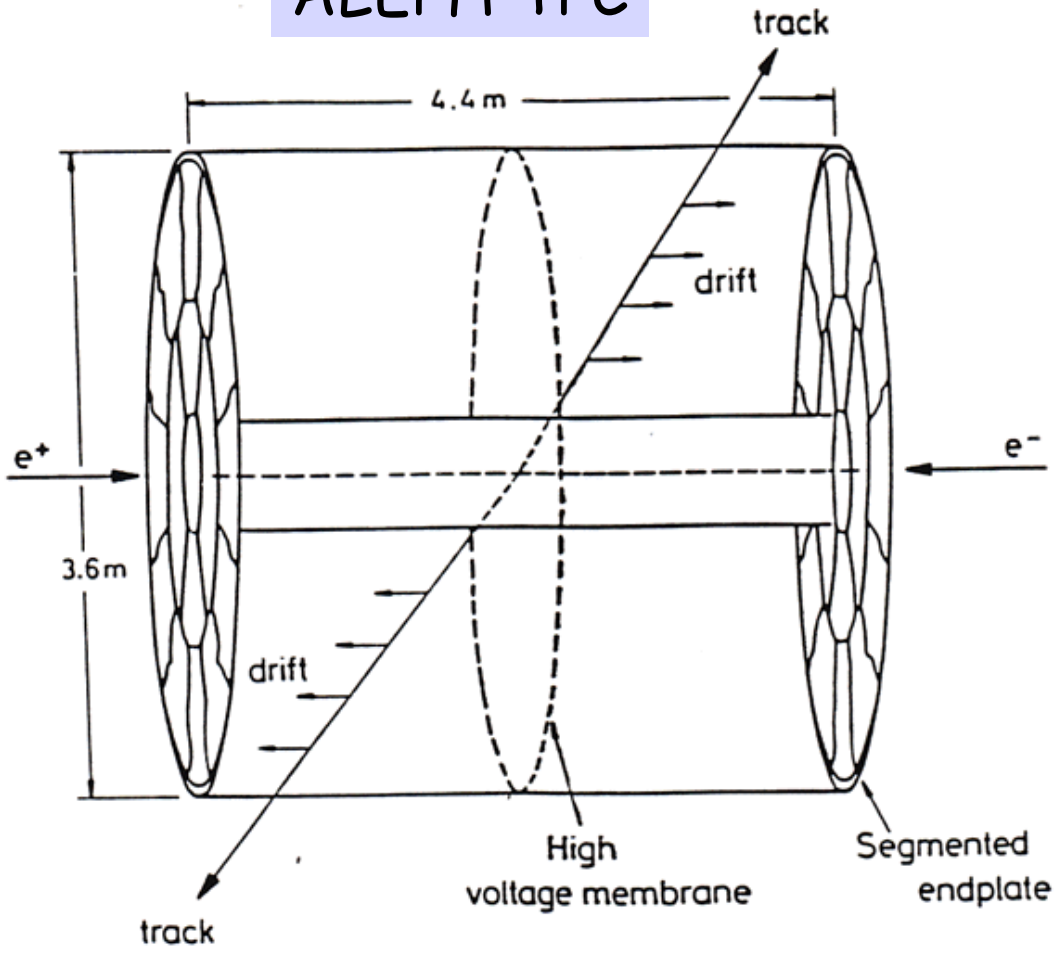

Cerenkov Counters

- Threshold detectors
- Differential detectors
- Ring Imaging detectors

Cerenkov Counters

- Part of the light emitted as a particle passes through a dielectric medium at a velocity exceeding the speed of light in the medium appears as a coherent wavefront

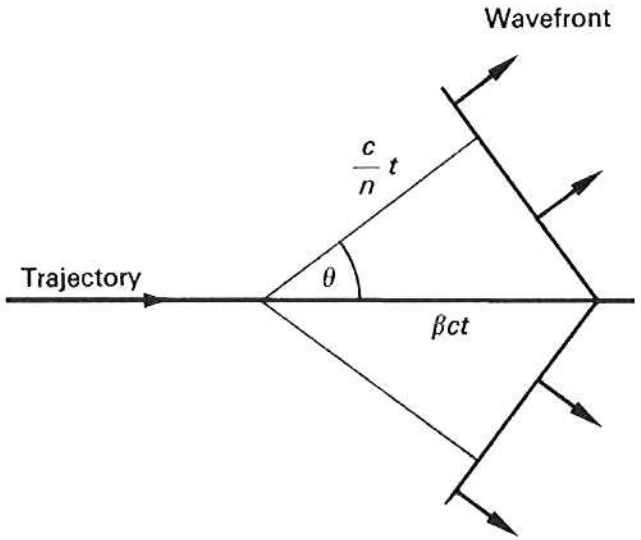

$$\cos\theta = \frac{ct/n}{\beta ct} = \frac{1}{\beta n}, \qquad \beta > \frac{1}{n}$$

Cerenkov Counters

- Cerenkov radiation

$$\frac{d^2N_\gamma}{dx\,dE} = \frac{\alpha z^2}{\hbar c}\left(1 - \frac{1}{\beta^2 n^2}\right)$$

- blue light predominates
  - well known blue glow from reactor
- Total rate of energy loss:

$$\frac{dW}{dx} = \frac{\alpha z^2}{\hbar c}\int\left(1 - \frac{1}{\beta^2 n^2}\right) E\,dE$$

$$= \frac{\alpha z^2}{2\hbar c}\left[(h\nu_1)^2 - (h\nu_2)^2\right]\left(1 - \frac{1}{\beta^2 n^2}\right)_{\text{av}}$$

  - a small fraction of the energy loss

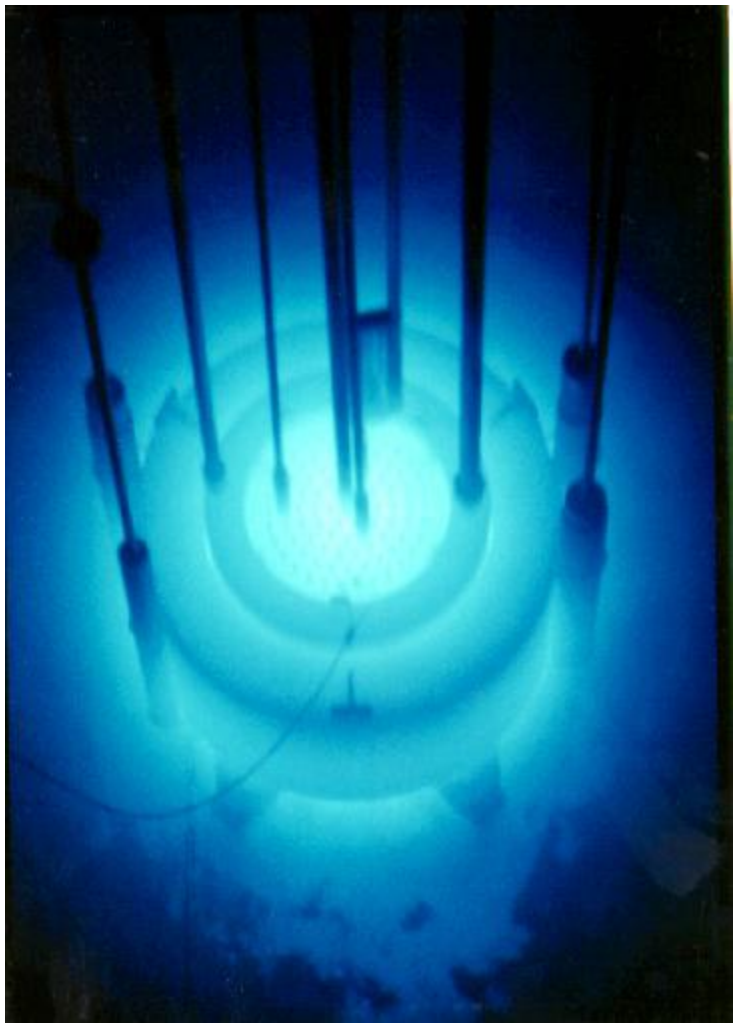

Cerenkov Counters

- The angle of emission of radiation is a measure of the velocity of the particle

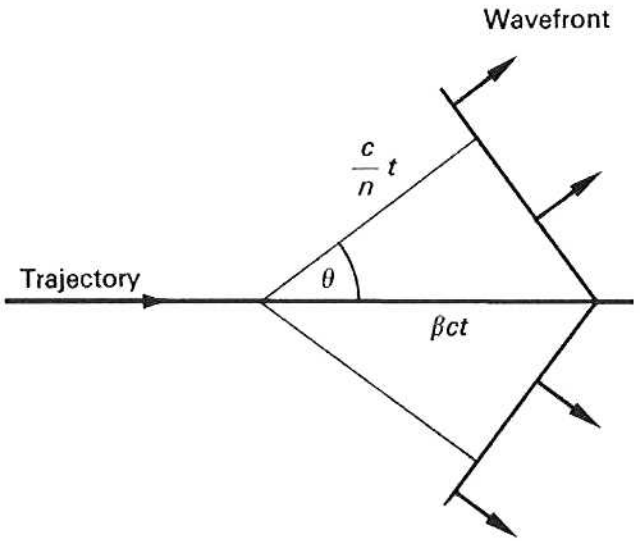

$$\cos\theta = \frac{ct/n}{\beta ct} = \frac{1}{\beta n}, \qquad \beta > \frac{1}{n}$$

Medium	$n-1$	γ (threshold)
helium (NTP)	3.3×10^{-5}	123
CO_2 (NTP)	4.3×10^{-4}	34
pentane (NTP)	1.7×10^{-3}	17.2
aerogel	$0.075 \rightarrow 0.025$	$2.7 \rightarrow 4.5$
H_2O	0.33	1.52
glass	$0.75 \rightarrow 0.46$	$1.22 \rightarrow 1.37$

Threshold Cerenkov Counters

- If two particles of different mass carry the same momentum, the lighter particle may emit Cerenkov radiation, while the heavier does not

•For example, in helium at NTP, the threshold for radiation is $\gamma = 123$

• A 100 GeV/c pion has a $\gamma \approx 700$, above the threshold while a 100 GeV/c proton has a $\gamma \approx 106$, below threshold

Medium	$n - 1$	γ (threshold)
helium (NTP)	3.3×10^{-5}	123
CO_2 (NTP)	4.3×10^{-4}	34
pentane (NTP)	1.7×10^{-3}	17.2
aerogel	$0.075 \rightarrow 0.025$	$2.7 \rightarrow 4.5$
H_2O	0.33	1.52
glass	$0.75 \rightarrow 0.46$	$1.22 \rightarrow 1.37$

Differential Cerenkov Counters

- Since the angle of emission of radiation is a measure of the velocity of the particle, by measuring the angle, one can determine velocity

$$\cos\theta = \frac{ct/n}{\beta ct} = \frac{1}{\beta n}, \qquad \beta > \frac{1}{n}$$

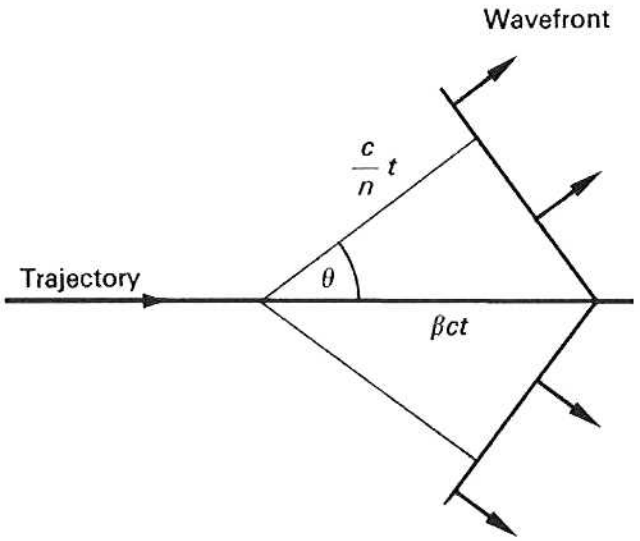

Medium	$n-1$	γ (threshold)
helium (NTP)	3.3×10^{-5}	123
CO_2 (NTP)	4.3×10^{-4}	34
pentane (NTP)	1.7×10^{-3}	17.2
aerogel	$0.075 \rightarrow 0.025$	$2.7 \rightarrow 4.5$
H_2O	0.33	1.52
glass	$0.75 \rightarrow 0.46$	$1.22 \rightarrow 1.37$

Ring Imaging Cerenkov Counters

- eg. SLD and DELPHI

  light at angle θ_c is focussed
  by mirror of radius R
  on ring CD

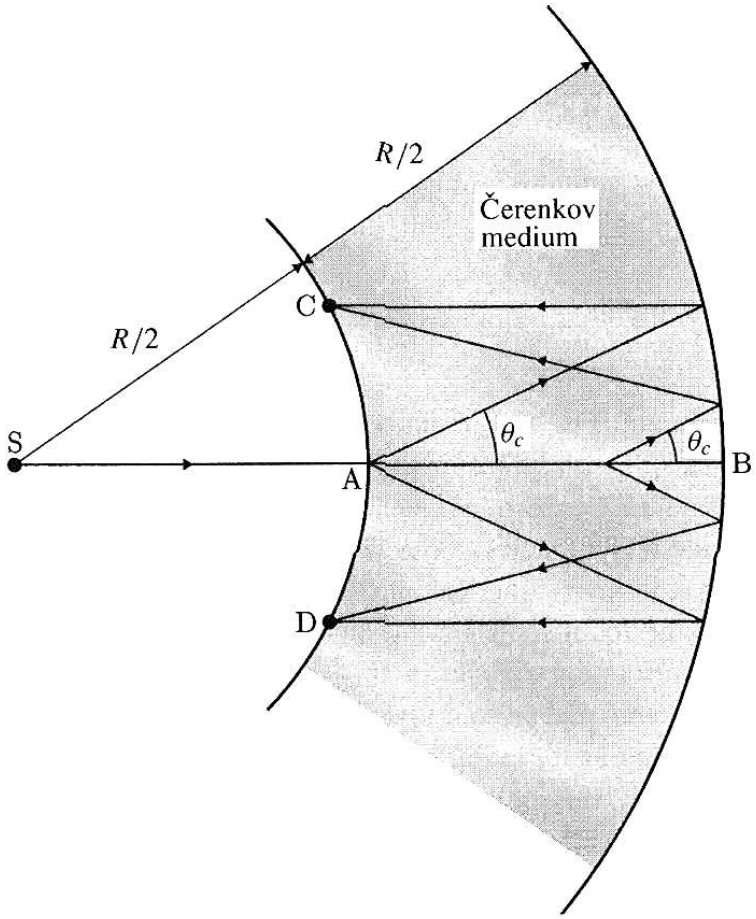

Ring Imaging Cerenkov Counters

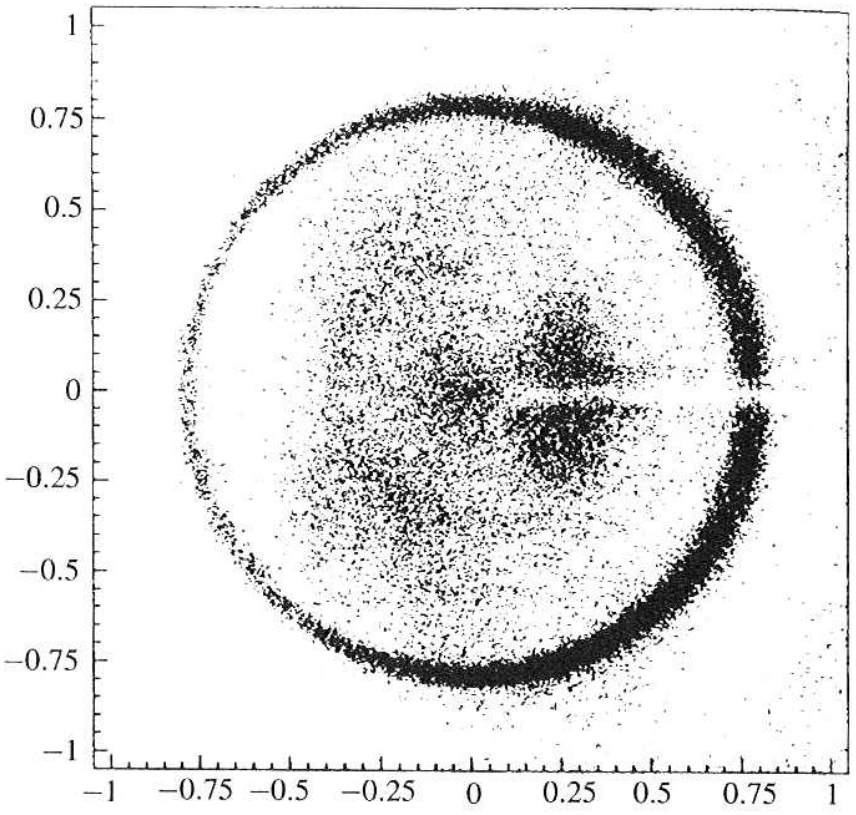

Muon in liquid (C_6F_{14})

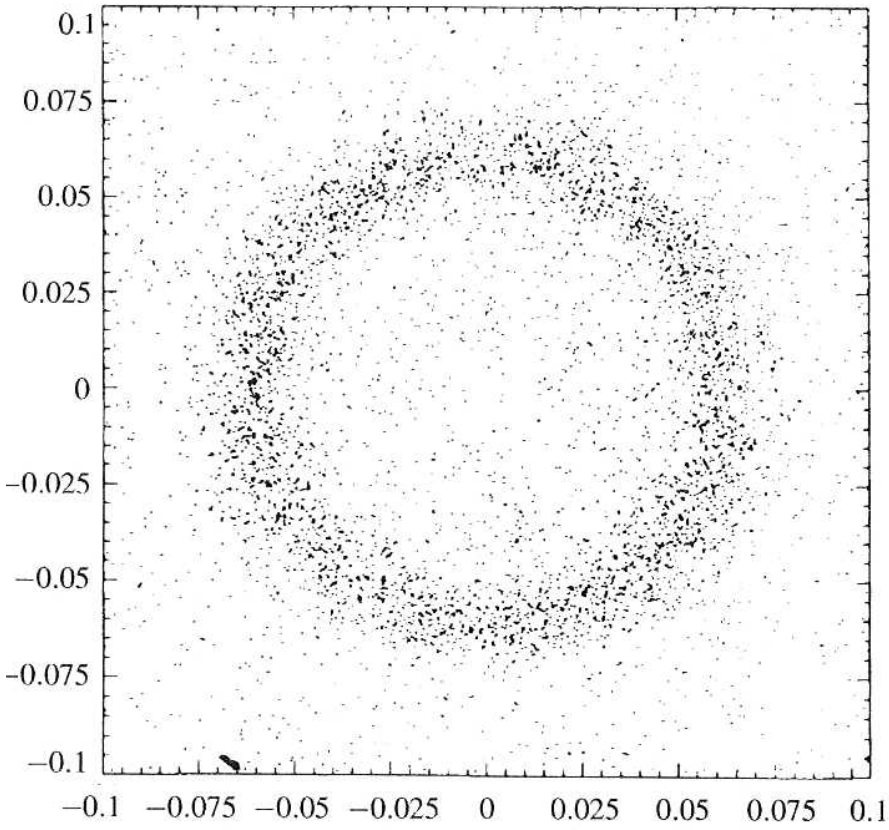

Muon in gas (87% C_5F_{12} 13% N_2)

Ring Imaging Cerenkov Counters

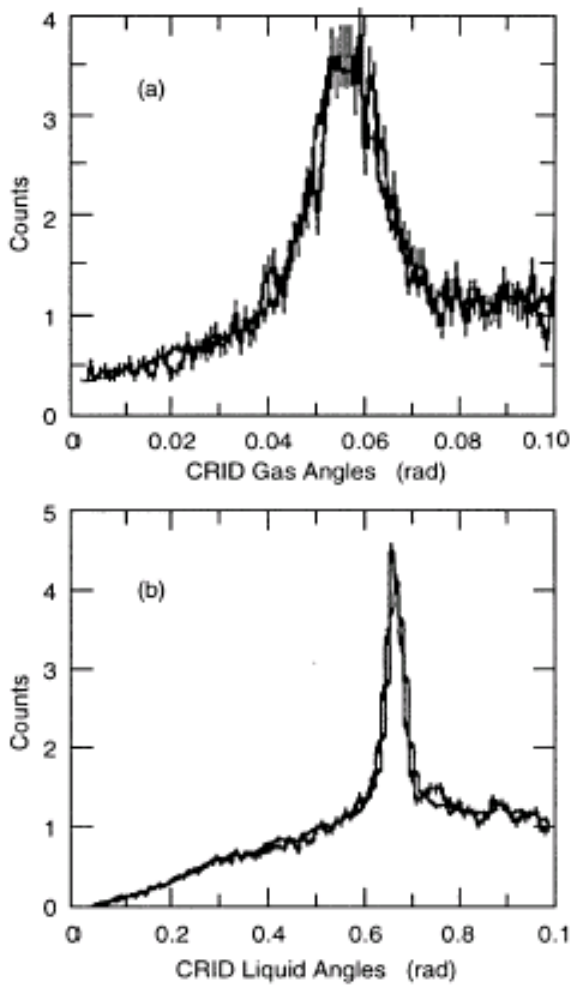

CRID final performance for gas and liquid rings for simple events such as di-muons [11]

Parameter	Gas rings	Liquid rings
Total fraction of photoelectrons contributing to the "final efficiency" compared to the "starting efficiency"	0.70	0.53
Mean photon energy (eV)	6.70	6.50
Mean refractive index	1.001646	1.27202
Mean Cherenkov angle (mrad) ($\beta = 1$ particle)	57.33	666.24
Calculated for radiator length (cm)	45	1
N_o [cm^{-1}]	80	42
Expected average number of photoelectrons per full ring ($\beta = 1$ particle) [11]	11–12	16
Measured average number of photoelectrons per full ring (di-muons) [34]	10	16–17

Solid State Detectors

- Silicon detectors in nuclear physics
- Microstrip detectors
- Hybrid pixels detectors
- Silicon drift detectors
- CCDs
- CMOS detectors
- Diamond detectors

Silicon Detectors

- Silicon detectors have several advantages over gas detectors
  - one major advantage is the small energy required to produce pair
    - 3.6 eV / electon-hole pair
    - 1.1 eV band-gap
  - excellent response time
    - few nanoseconds
  - many years of use in nuclear physics
    - position localization accuracy of 5 μm in one coordinate
    - two-track separation down to 10 μm
    - geometrical accuracy in the region of 1 μm
    - bias voltages less than 100 V for microstrip detectors
    - time response less than 5 ns
    - relatively simple installation.

Silicon Detectors

- Theory of silicon junction
  - depleted region is the region where the free carriers have been removed
  - electron-hole pairs created in the depletion region will be swept out by the bias voltage

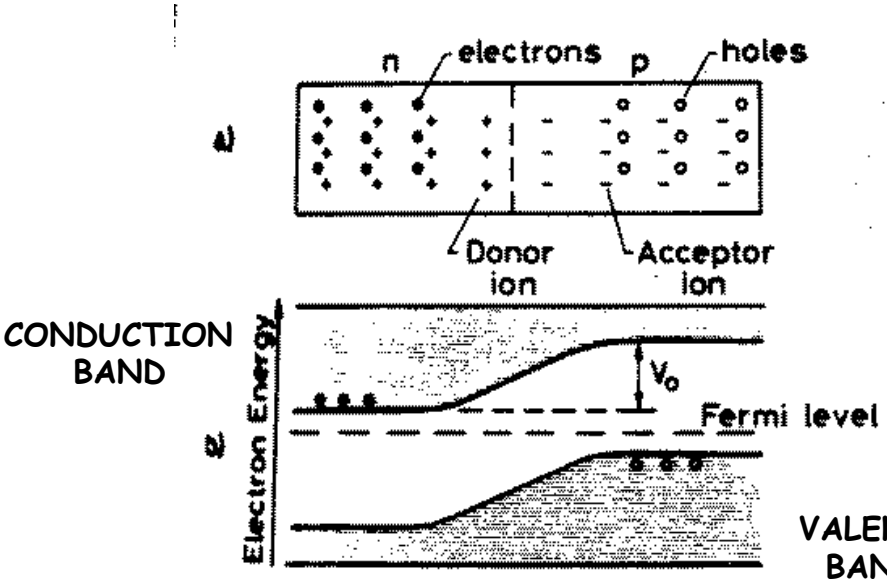

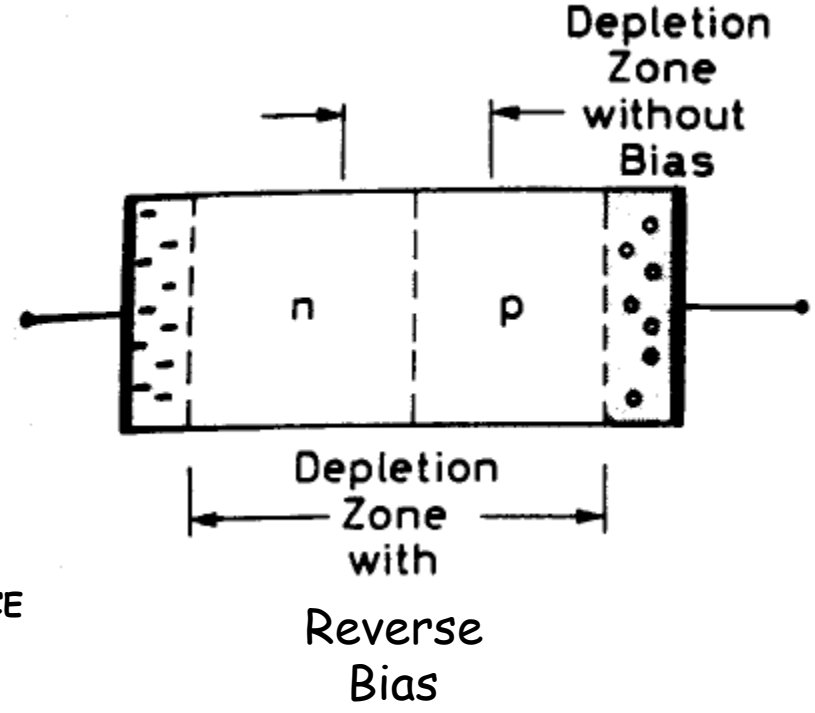

Silicon Detectors

- Theory of silicon junction
  - The thickness of the depletion depth is

$$d = 0.5\ \mu m\ \sqrt{\rho(\Omega cm)}\ V(volts)$$

  - Therefore, for large depletion depth with moderate voltage, need high resistivity, ~ 2-5 k Ωcm

$$d = 0.5\ \mu m\ \sqrt{\rho(\Omega cm)}\ V(volts)$$

$$d = 0.5\ \mu m\ \sqrt{4 \times 10^3}\ 100$$

$$d \approx 300\ \mu m$$

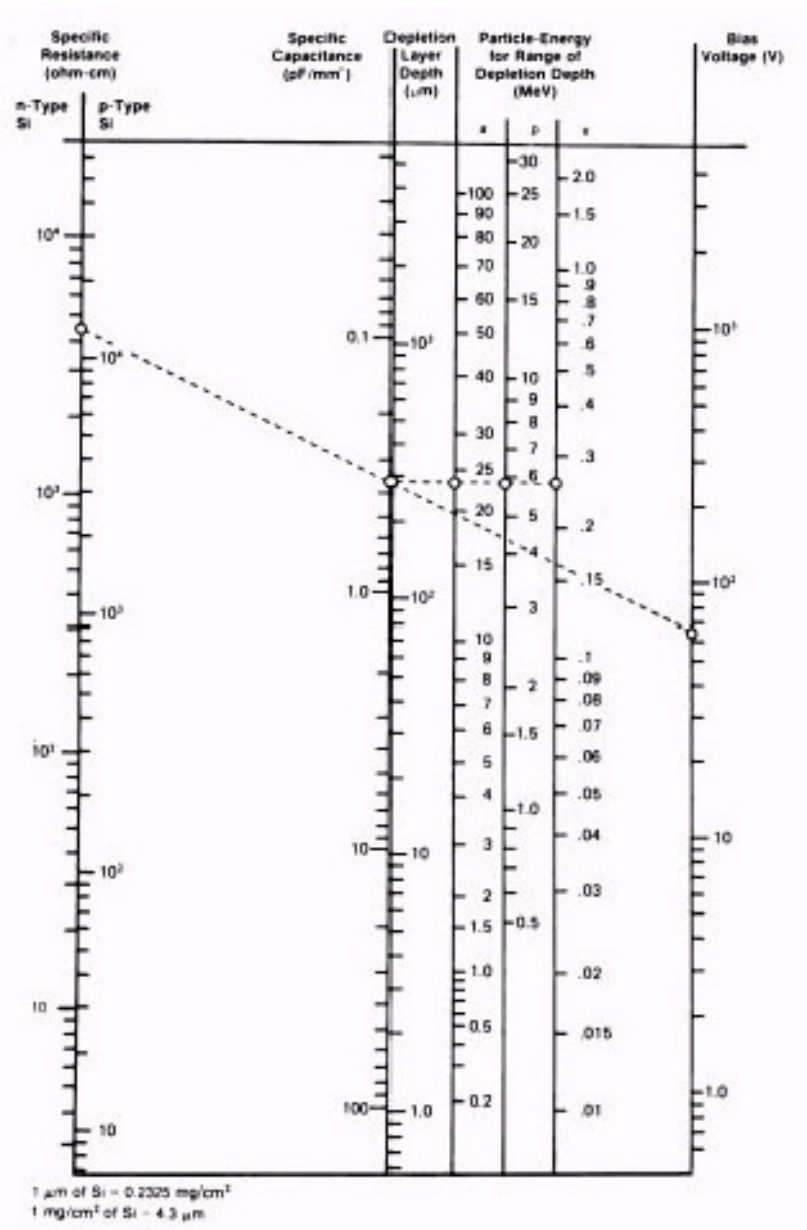

A straight edge intersecting the center vertical line at the required depletion depth will give combinations of resistivity and detector bias that may be used to achieve that depth. (Shown, for example, is the voltage that must be applied to a 13,000 Ω-cm p-type or 4500 Ω-cm n-type silicon detector to stop a 23-MeV alpha, a 6-MeV proton, or a 250-keV electron within the depletion depth.)

Silicon Detectors

- Blankenship Nomogram
  - IEEE Trans NS7, 190 (1960)

Silicon Microstrip Detectors

- 1980 - Kemmer introduced planar technology
- Outstanding performance has since been achieved with microstrip detectors

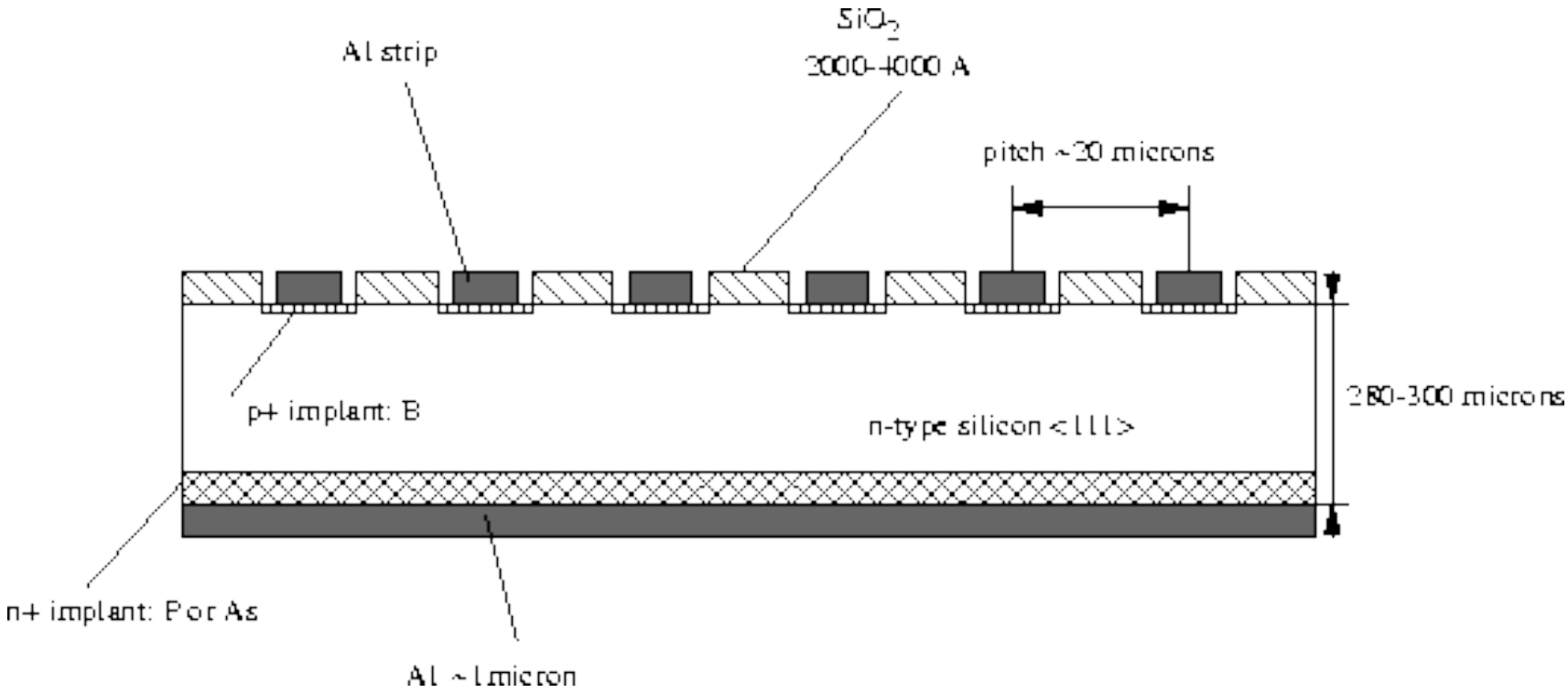

Silicon Microstrip Detectors

- Star ladder construction

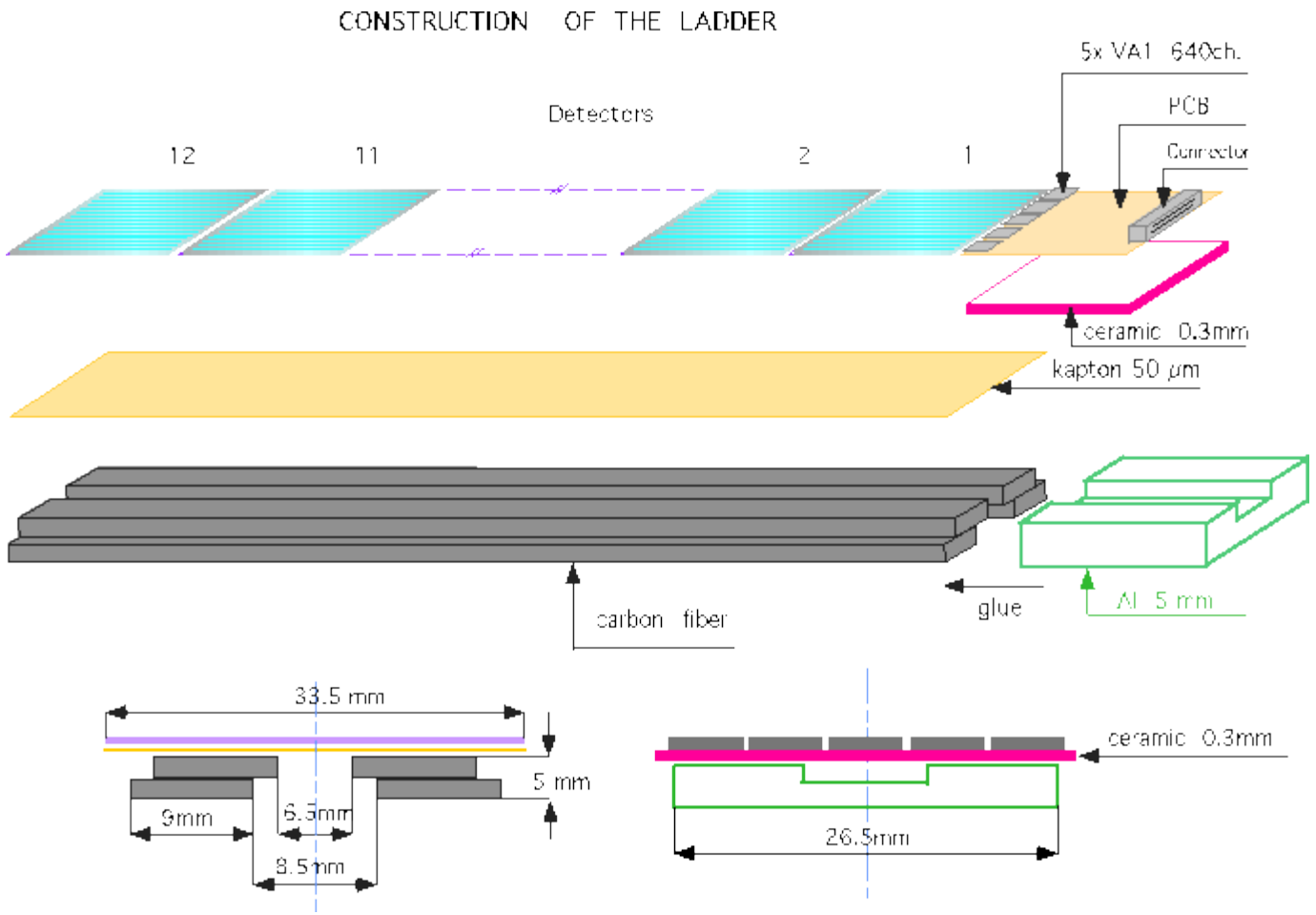

Hybrid Pixel Detectors

- Pixel detectors are 2D detectors

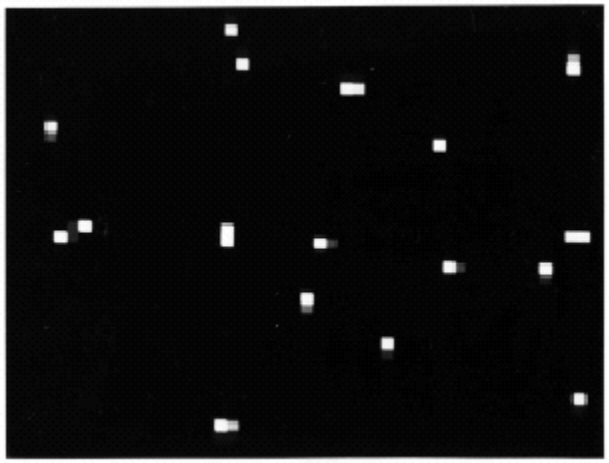

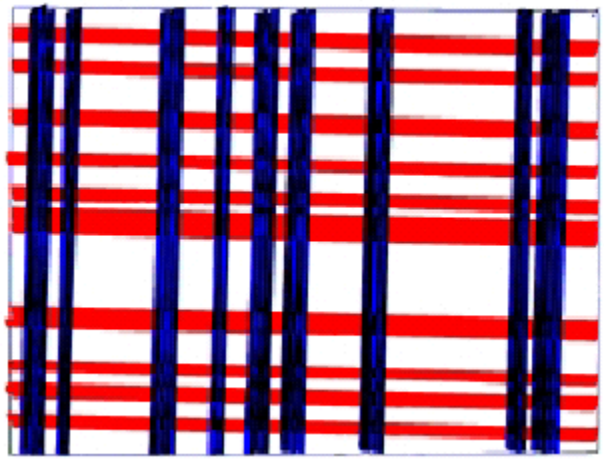

- Great reduction in ambiguities

Hybrid Pixel Detectors

- Hybrid pixel detectors have been developed for LHC
  - rad hard
  - fast
  - high background rate near IP rules out microstrips

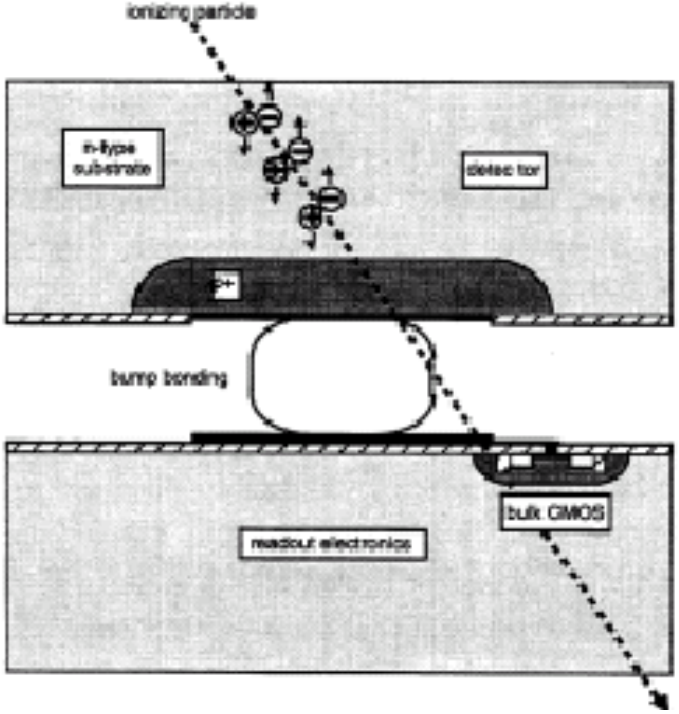

Disadvantages
- large power consumption
- large pixel sizes
- thick devices (multiple scatt)
  (compared to CCDs)